

AD-A235 863



WRDC-TR-90-4103

DTIC
ELECTE
MAY 5 1991



XDTM Reinforced Beryllium-Based Composites

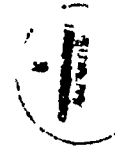
Wendell Meyerer, Al Bopp (Martin Marietta), Fritz Gensing (Brush Wellman)
Martin Marietta Corporation
Martin Marietta Missile Systems
P.O. Box 555837
Orlando, FL 32855-5837

December 1990

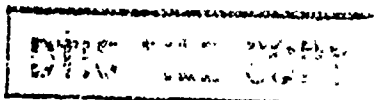
Final Report for Period March 1989 - August 1990

Accession For	
NTIS GRA&I	<input checked="" type="checkbox"/>
DTIC Inf	<input type="checkbox"/>
Unannounced	<input type="checkbox"/>
Justification	
by _____	
Distribution _____	
Availability Codes	
Availability _____	
Dist	Special
A-1	

Approved for public release; distribution is unlimited



Materials Laboratory
Wright Research and Development Center
Air Force Systems Command
Wright-Patterson Air Force Base, Ohio 45433-6533



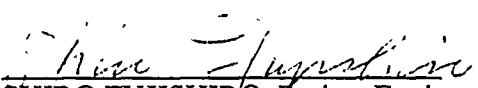
91 5. 13 012

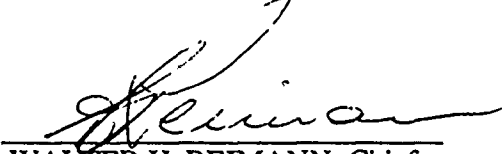
NOTICE

When Government drawings, specifications, or other data are used for any purpose other than in connection with a definitely Government-related procurement, the United States Government incurs no responsibility or any obligation whatsoever. The fact that the government may have formulated or in any way supplied the said drawings, specifications, or other data, is not to be regarded by implication, or otherwise in any manner construed, as licensing the holder, or any other person or corporation; or as conveying any rights or permission to manufacture, use, or sell any patented invention that may in any way be related thereto.

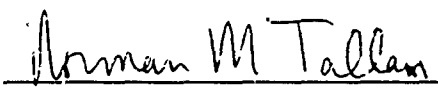
This report is releasable to the National Technical Information Service (NTIS). At NTIS, it will be available to the general public, including foreign nations.

This technical report has been reviewed and is approved for publication.


SHIRO FUJISHIRO, Project Engineer
Materials Development Branch
Metals and Ceramics Division


WALTER H. REIMANN, Chief
Materials Development Branch
Metals and Ceramics Division

FOR THE COMMANDER


NORMAN M. TALLAN, Director
Metals and Ceramics Division
Materials Directorate

If your address has changed, if you wish to be removed from our mailing list, or if the addressee is no longer employed by your organization, please notify WL/MLLM, WPAFB, OH 45433-6533 to help us maintain a current mailing list.

Copies of this report should not be returned unless return is required by security considerations, contractual obligations, or notice on a specific document.

REPORT DOCUMENTATION PAGE				Form Approved OMB No. 0704-0188	
1a. REPORT SECURITY CLASSIFICATION Unclassified		1b. RESTRICTIVE MARKINGS N/A			
2a. SECURITY CLASSIFICATION AUTHORITY N/A		3. DISTRIBUTION / AVAILABILITY OF REPORT Approved for public release; distribution is unlimited			
2b. DECLASSIFICATION / DOWNGRADING SCHEDULE N/A					
4. PERFORMING ORGANIZATION REPORT NUMBER(S) OR-20,099		5. MONITORING ORGANIZATION REPORT NUMBER(S) WRDC-TR-90-4103			
6a. NAME OF PERFORMING ORGANIZATION Martin Marietta Corporation Martin Marietta Missile Systems		6b. OFFICE SYMBOL <i>(if applicable)</i>	7a. NAME OF MONITORING ORGANIZATION Wright Research and Development Center Materials Laboratory (WRDC/MLLS)		
6c. ADDRESS (City, State, and ZIP Code) P.O. Box 555837 Orlando, FL 32855-5837		7b. ADDRESS (City, State, and ZIP Code) Wright-Patterson AFB OH 45433-6533			
8a. NAME OF FUNDING / SPONSORING ORGANIZATION		8b. OFFICE SYMBOL <i>(if applicable)</i>	9. PROCUREMENT INSTRUMENT IDENTIFICATION NUMBER F33615-89-C-5614		
8c. ADDRESS (City, State, and ZIP Code)		10. SOURCE OF FUNDING NUMBERS			
		PROGRAM ELEMENT NO. 61101F	PROJECT NO. ILIR	TASK NO. 02	WORK UNIT ACCESSION NO. 12
11. TITLE (Include Security Classification) XDTM Reinforced Beryllium-Based Composites					
12. PERSONAL AUTHOR(S) Wendell Meyerer, Al Bopp, Fritz Gensing					
13a. TYPE OF REPORT Final		13b. TIME COVERED FROM Mar 89 TO Aug 90	14. DATE OF REPORT (Year, Month, Day) December 1990		15. PAGE COUNT 74
16. SUPPLEMENTARY NOTATION					
17. COSATI CODES			18. SUBJECT TERMS (Continue on reverse if necessary and identify by block number) Beryllium, XDTM, Composites, Beryllium Castings, Dispensoids, Grain Refinement		
FIELD	GROUP	SUB-GROUP			
			19. ABSTRACT (Continue on reverse if necessary and identify by block number) <p>Eleven beryllium castings were made by Brush Wellman using dispersoid materials provided by Martin Marietta Laboratories. Eight castings had a beryllium matrix, while three had a NiBe matrix. Each casting was analyzed metallographically. It was found that all the selected dispersoid materials reacted with the beryllium matrix. Little grain refinement was observed in the castings. Slabs cut from the cast billets were rolled to Produce sheet. It was found that the grain size of the rolled material was only slightly finer than a pure Be control sample.</p>		
20. DISTRIBUTION / AVAILABILITY OF ABSTRACT <input checked="" type="checkbox"/> UNCLASSIFIED/UNLIMITED <input type="checkbox"/> SAME AS RPT <input type="checkbox"/> DTIC USERS			21. ABSTRACT SECURITY CLASSIFICATION Unclassified		
22a. NAME OF RESPONSIBLE INDIVIDUAL Shiro Fujishiro		22b. TELEPHONE (Include Area Code) 513-255-1320		22c. OFFICE SYMBOL WRDC/MLLS	

FOREWORD

This is the final technical report covering work performed under contract F33615-89-C-5614 for the period from March 1985 through August 1990. This program was conducted under the cognizance of Capt E. Robertson and Dr Shiro Fujishiro at the Materials Laboratory, Wright Laboratory, Wright-Patterson Air Force Base, Ohio.

The report was prepared by Martin Marietta Missile Systems, Orlando, Florida, as prime contractor. Mr Wendell J. Meyerer was the program manager. Major subcontractors on this program and contributors to this report are Martin Marietta Laboratories, Baltimore, Maryland, and Brush Wellman, Elmore, Ohio. Dr Al Bopp (Martin Marietta Laboratories) and Mr R. Fritz Gensing (Brush Wellman) were the program managers at the respective subcontractors' facilities.

CONTENTS

	<u>Page</u>
FOREWORD	iv
SUMMARY	vi
LIST OF TABLES	vii
LIST OF FIGURES	viii
I. INTRODUCTION	1
A. Grain Size Reduction in XD Composites	5
B. Materials and Process Option	6
C. Thermodynamic Analysis	7
II. EXPERIMENTAL PROCEDURE	14
A. Casting	17
B. Cross-Rolling	17
C. Microstructure	23
D. Pole Figures	23
E. Mechanical Testing	24
III. RESULTS AND DISCUSSION	25
A. Casting Be-0: Beryllium Control Sample	25
B. Casting Be-1: 10-Weight-Percent TiC in Cu with Be Matrix	25
C. Casting Be-2: 10-Weight-Percent Ti_5Si_3 in Cu with a Be Matrix	29
D. Casting Be-3: 6-Weight-Percent Ti_5Si_3 in Ni with a Be Matrix	44
E. Casting Be-4: 10-Weight-Percent TiO_2 in Cu with a Be Matrix	44
F. Casting Be-5: 10-Weight-Percent Ti_5Si_3 in Ti with a Be Matrix	49
G. Casting Be-9: 10-Weight-Percent $MoSi_2$ in Cu with a Be Matrix	54
H. Casting Be-10: 10-Weight-Percent CoAl in Cu with a Be Matrix	59
I. Casting Be-6: Beta-NiBe Control	66
J. Casting Be-7: 10-Weight-Percent Ti_5Si_3 in Cu with a Beta-NiBe Matrix	66
K. Casting Be-8: 10-Weight-Percent Ti_5Si_3 in Ni with a Beta-NiBe Matrix	69
IV. CONCLUSIONS	72
REFERENCES	74

SUMMARY

Eleven beryllium castings were made by Brush Wellman using dispersoid materials provided by Martin Marietta Laboratories. Eight castings had a beryllium matrix, while three had a NiBe matrix. Each casting was analyzed metallographically. It was found that all the selected dispersoid materials reacted with the beryllium matrix. Little grain refinement was observed in the castings. Slabs cut from the cast billets were rolled to Produce sheet. It was found that the grain size of the rolled material was only slightly finer than a pure Be control sample.

TABLES

<u>Table</u>		<u>Page</u>
1	Free Energies for Stability Calculations	12
2	XD-2e Master Alloys List	15
3	Master Alloy Materials	15
4	Billet Designations, Dispersoid and Carrier Materials . .	18
5	Rolling Schedule for XD Beryllium Cross-Rolled Blocks . .	20
6	Rolled Specimen Inventory and Status	22
7	Tensile Test Results	22

FIGURES

<u>Figure</u>		<u>Page</u>
1	Castable Beryllium program schedule	2
2	Free energy as a function of temperature for chemical reactions between molten Be and an XD Ti_5Si_3 master alloy	13
3	Macrographs of as-cast billets Be-6 and Be-10, with large shrinkage pores in both castings	19
4	Macrographs of rolled billets with billet numbers below each billet and pack numbers indicated on several of the sheets	21
5	As-cast Be-0	26
6	Cross-rolled Be-0	27
7	Pole figure for Be-0	28
8	Scanning electron micrograph (a) and X-ray diffraction pattern (b1 and b2) of a $TiC + Cu$ (35-weight-percent) master alloy (Be-1), 10,000X . . .	30
9	As-cast Be-1: 10-weight-percent TiC in Cu with a Be matrix	32
10	Spectra from angular particles (identified as Be_2C) in as-cast Be-1, with Cu and Ti resulting from the matrix	33
11	SEM micrographs of the Ti-rich phase in Be-1	34
12	Microstructure of cross-rolled Be-1 sheet	35
13	Scanning electron micrograph (a) and X-ray diffraction pattern (b1 and b2) of a $Ti_5Si_3 + Cu$ (33-weight-percent) master alloy (Be-2), 10,000X . . .	37
14	As-cast Be-2: 10-weight-percent Ti_5Si_3 in Cu with a Be matrix	39
15	X-ray dot maps from the Ti-rich phase in casting Be-2	40
16	X-ray spectra of particles in billet Be-2	41
17	Microstructure of cross-rolled Be-2	42
18	Si regions and cracked Ti-rich particles in Be-2 sheet	43

FIGURES (Continued)

<u>Figure</u>		<u>Page</u>
19	Scanning electron micrograph (a) and X-ray diffraction pattern (b1 and b2) of Ti_5Si_3 + Ni (33-weight-percent) master alloy (Be-3), 1000X	45
20	As-cast Be-3: 6-weight-percent Ti_5Si_3 in Ni with a Be matrix	47
21	Microstructure of cross-rolled Be-3	48
22	Scanning electron micrograph (a) and X-ray diffraction pattern (b1 and b2) of a TiO_2 + Cu master alloy (Be-5), 100X	50
23	Be-4: 10-weight-percent TiO_2 in Cu with a Be matrix, as-cast and rolled	52
24	X-ray diffraction pattern for the Ti_5Si_3 + Ti (33-weight-percent) master alloy (Be-4)	53
25	Be-5: 10-weight-percent Ti_5Si_3 in Ti with a Be matrix, as-cast and rolled	55
26	Scanning electron micrograph (a) and X-ray diffraction pattern (b) of a $MoSi_2$ + Cu (50-weight-percent) master alloy (Be-6), 2000X	56
27	Scanning electron micrograph (a) and X-ray diffraction pattern (b) of a $MoSi_2$ + Cu (65-weight-percent) master alloy (Be-10), 2000X	57
28	As-cast Be-9: 10-weight-percent $MoSi_2$ in Cu with a Be matrix	58
29	Pole figure for Be-9	60
30	Microstructure of cross-rolled Be-9	61
31	Scanning electron micrograph (a) and X-ray diffraction pattern (b1 and b2) of a CoAl + Cu (50-weight-percent) master alloy (Be-12), 2000X	62
32	As-cast Be-10: 10-weight-percent CoAl in Cu with a Be matrix	64
33	Microstructure of cross-rolled Be-10	65
34	Be-6: NiBe, as-cast and rolled	67

FIGURES (Concluded)

<u>Figure</u>		<u>Page</u>
35	As-cast Be-7: 10-weight-percent Ti_5Si_3 in Cu with a NiBe matrix	68
36	Scanning electron micrograph (a) and X-ray diffraction pattern (b) of a Ti_5Si_3 + Ni (70-weight-percent) master alloy (Be-9), 1000X	70
37	As-cast Be-8: 10-weight-percent Ti_5Si_3 in Ni with a NiBe matrix	71

I. INTRODUCTION

The objective of this program is to demonstrate the feasibility of using fine-particle inoculants called dispersoids, generated by Martin Marietta using its proprietary XD process, to produce fine-grained beryllium castings. Such castings would be much less expensive than beryllium-based materials produced by conventional powder metallurgy. The schedule for this program is shown in Figure 1.

Beryllium is an extremely attractive candidate for lightweight aerospace applications. It has a higher melting temperature and greater tensile strength than either magnesium or aluminum, a higher strength-to-weight ratio than either metal, and a lower thermal coefficient of expansion and higher specific heat. Its modulus of elasticity is four times that of aluminum.

The low density and high modulus of beryllium and beryllium-based intermetallics make them ideal materials for aerospace applications requiring high dimensional stability and low weight. Conventional beryllium-based materials are produced by powder metallurgy processes, because the large grains that form in beryllium during solidification decrease the strength and ductility of the material. Grain growth, although normally slow, can accelerate as any metal approaches its melting point. Be is no exception, showing rapid grain growth above 900°C. Be also has a high enthalpy of fusion (2.33 kcal/mole), so grain growth in melt-processed Be can also be driven by the energy released during solidification. A further contributing factor is the alpha-beta allotropic transition (1270°C), which has a comparatively large associated enthalpy (0.61 kcal/mole) that adds yet another energy increment at high temperatures. These energy additions in a critical temperature regime activate grain growth.

MARTIN MARIETTA MISSILE SYSTEMS
 CASTABLE BERYLLIUM
 PROGRAM SCHEDULE

JUN 01, 1990
 R & T PLANNING

F33615-89-C-5614, PM: W. Meyerer, ext. 4208
 1990

DEVELOPMENT OF CASTABLE
 X-D BERYLLIUM

CONTRACT AWARD 3/31/89
 REVIEWS

PHASE I
 PRELIMINARY STUDIES:

Thermodynamic Studies/
 Literature Search
 Recommendations

Sponsor Approval

PHASE II
 X-D BERYLLIUM DEMO:

Sample Preparation
 Evaluation

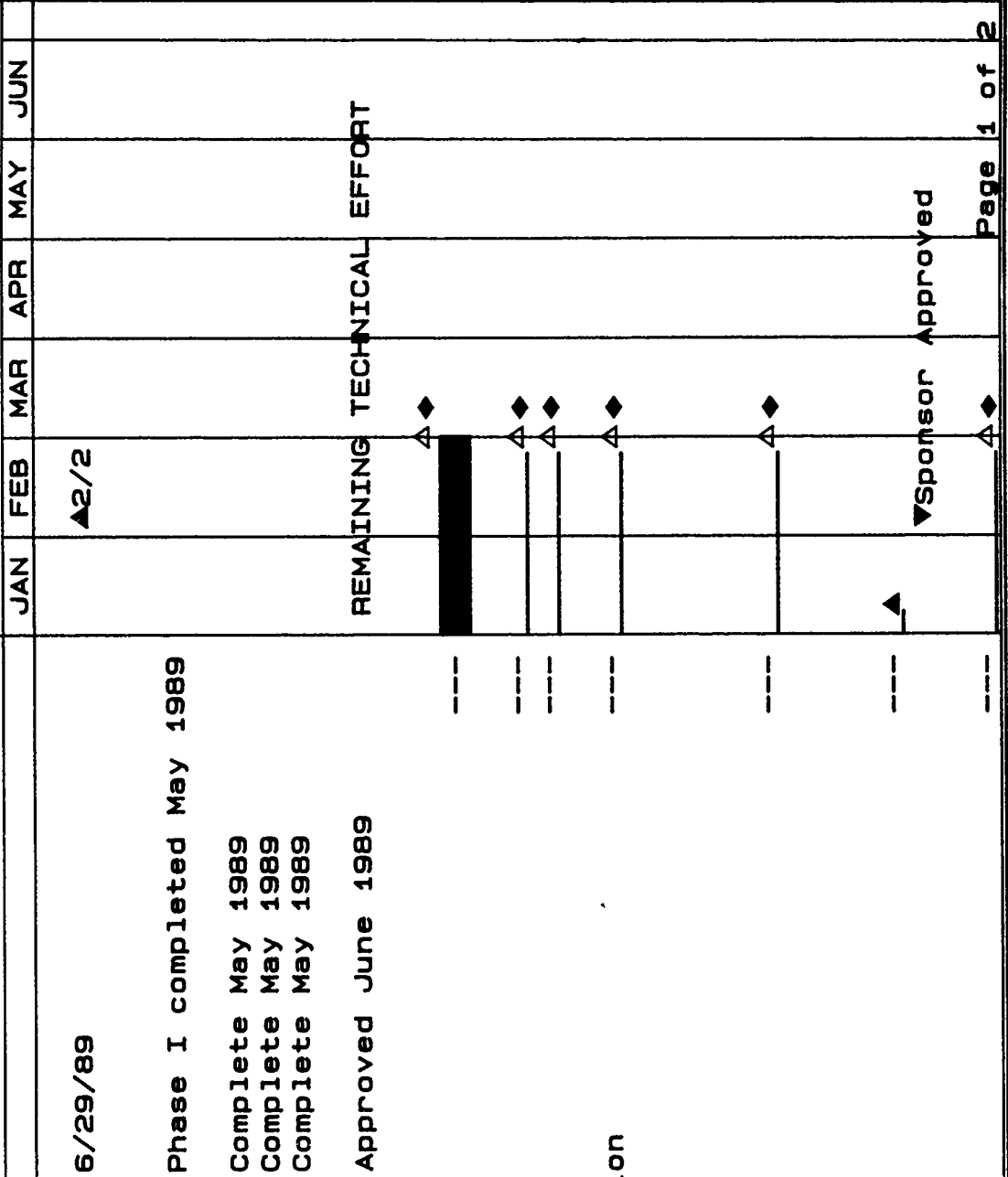
Characterize Dispersion

Chemistry
 Volume & Dispr
 Synthesis Proc

Characterize Matrix
 Composition
 Metallograph Exam

Characterize Proc
 Casting Method

Mechanical Eval



Page 1 of 2

Figure 1. Castable Beryllium program schedule.

DEVELOPMENT OF CASTABLE X-D BERYLLIUM		MARTIN MARIETTA MISSILE SYSTEMS CASTABLE BERYLLIUM PROGRAM SCHEDULE													JUN 01, 1990 R & T PLANNING					
		F33615-89-C-5614, PM: W. Meyerer, ext. 4208																		
		1989												1990						
		M	A	M	J	J	A	S	O	N	D	J	F	M	A	M	J	J	A	S
CONTRACT AWARD																				
CONTRACT MODIFICATIONS		▲3/31/89								▲P00001 4/21/89						▲P00002 11/21/89			▲P00003 4/25/90	
DELIVERABLE DATA:																				
1. Progress Report			▲	▲	▲	▲	▲		▲		▲									
2. Experimental Plan				▲	▲	▲														
3. Contractor's Voucher			▲	▲	▲	▲	▲		▲		▲									
4. System Safety/Hazard Analysis Report					▲	▲	▲													
5. OHH. Assessment Rpt					▲	▲	▲													
6. Presentation Mtrls					▲	▲	▲													
7. Final Technical Rpt:																				
Draft																				
Govt Approval																				
Final																				

Draft Due 4/20
▲

GA
7/20

▲ Final
8/20

Figure 1. (continued)

Because there are no acceptable casting technologies to produce beryllium components, consolidated powder metal billets are machined to produce components. During comminution, the Be powder rapidly develops an oxide coating that acts as a barrier and is stable at high temperatures. The BeO on the particle surface stabilizes the grain size, and a high level of refinement is achievable. However, oxygen levels of 1 percent are common, and powder processing is inherently expensive. Material cost is further increased by the toxicity of Be and BeO dust, which makes expensive containment equipment necessary. The development of a casting technology that produces a fine-grained and ductile beryllium matrix would offer substantial cost savings over this conventional processing technique.

Because the mechanical properties of beryllium follow a Hall-Petch relationship, extensive efforts have been expended on reducing the grain size of as-cast Be. Those efforts have yielded these findings and results:

- o The development of grains during solidification is dependent on purity. Impurities rejected from the solidified Be broaden the freezing range of the remaining liquid, thus resulting in large grains.

- o Various cold working techniques have been successfully used to reduce the grain size of Be. (Hot work cannot be applied because of grain growth, as discussed above.) Upset forging has been shown to improve the mechanical properties of cast Be as a direct result of grain refinement.² Rolling has been shown to produce high strength material in the sheet; however, through-thickness properties are not as impressive.

- o The high intrinsic viscosity of molten Be makes the use of inoculants impractical. In powdered-metal-produced materials, the addition of hard second-phase particles limited the grain size and increased strength, but low-temperature ductility did not improve accordingly.³

Despite the difficulties encountered in attempting to reduce the grain size of as-cast Be, the recent successes of Martin Marietta's XD TM process served as an impetus for this program. The remainder of this report discusses the CD process, how it was used in this program, and the results.

A. GRAIN SIZE REDUCTION IN XD COMPOSITES

XD is a process for introducing fine (typically micrometer) ceramic particles, or dispersoids, into metal or intermetallic matrix. Because the dispersoids are synthesized directly in a matrix, they are not exposed to air and hence have a surface free of oxide coatings. This "clean" surface enhances wetting between the two phases and provides stability to the composite. In addition, particles are formed throughout the matrix, leading to a uniform dispersion. Lastly, the size of the ceramic dispersoid particles can be manipulated, within limits, by the starting materials and process conditions.

The generic nature of the process has been demonstrated in numerous metal matrices ranging from aluminum to copper and in titanium-aluminide and nickel-aluminide intermetallics. Both DoD agencies and NASA have shown significant interest in XD technology. Contracts have included efforts in nickel aluminides (ONR), titanium aluminides (DARPA/NRL), aluminum (NASA), copper (NASP/JPO), and this effort with beryllium.

From extensive experience with aluminum and titanium-aluminide matrices, Martin Marietta Laboratories understands the criteria for microstructure refinement via CD composites. Mechanistically, the particles act to impede the motion of grain boundaries during solidification. Grain refinement is matrix-dependent and has been found to be a function of both dispersoid size and loading. Grain size has been found to be indifferent to the chemistry of the dispersoid as long as it is chemically stable in and wetted by the melt. Therefore, the logic behind applying XD to Be was to identify dispersoids that were chemically stable in molten Be and were of the critical size needed to inhibit the motion of grain boundaries during solidification.

The dispersoid material, a billet of prereacted elemental powder, contains a dispersion of fine inoculant particles in a carrier matrix. When added to the melt, the carrier dissolves, releasing the particles. Depending on reactivity, the particles may interact chemically with the melt. Upon solidification, the particles act as inoculants and increase the rate of grain nucleation. In the solidified material, the particles act as a dispersed compositing agent.

Eleven beryllium castings were made by Brush Wellman using dispersoids provided by Martin Marietta. The composition and morphology of the castings were characterized after each step to determine the effects of the beryllium environment on the dispersoids. Early program results were transmitted to Martin Marietta to confirm their thermodynamic calculations and refine their model. Dispersoids and inoculants were then selected for later castings.

B. MATERIALS AND PROCESS OPTIONS

The solubility of most elements in Be is extremely limited, so alloying is not a viable approach for regulating Be's mechanical and physical properties as it is with most metals. Moreover, molten Be is highly reactive and dissolves or forms intermetallic compounds with most metals. By analogy, Ti is likewise highly reactive and likewise tends to form intermetallics. However, experience has shown that Ti can be made less reactive by conversion to an aluminide intermetallic. For example, TiB_2 dissolves in Ti and forms TiB. However, in Y-TiAl, TiB_2 is stable. Continuing the logic, one approach might be to lower the reactivity of Be by conversion to a beryllide.

Appreciating that molten Be is highly reactive and thermodynamically favors solutions and intermetallics, the approach to the beryllium system was based on four options:

- o $TiBe_x$ as reinforcement. As a terminal beryllide, $TiBe_{12}$ is thermodynamically stable in Be. Although chemically stable, prior work with rapidly solidified terminal beryllides showed such phases do not lead to grain refinement.
- o Other intermetallics as dispersoids. An intermetallic will not react with Be if it is more stable than its "conjugate" beryllide. For example, $CoAl$ will not be driven to form $CoBe$ if the aluminide has lower free energy.
- o Beryllides as the matrix phase. Beryllides are more stable than Be and are thus expected to be less chemically aggressive (recall the $Ti/TiAl$ analogy). In addition, certain beryllides are also interesting materials.
- o Ceramic dispersoids. A ceramic phase that is stable in Be may exist.

This approach of attacking the problem from multiple directions was proposed to maximize the probability of identifying stable phases and to provide insight into the chemistry of Be composites. To identify reasonable candidates, a thermodynamic analysis of numerous Be-based composites was pursued, as discussed below.

C. THERMODYNAMIC ANALYSIS

The object of the thermodynamic analysis was to predict stable composite systems. The findings from these analyses were used to guide the selection of materials for experimental study. The predicted stable systems were then prepared and analyzed to demonstrate the utility of both the thermochemical techniques and the XD process (see Section II, Experimental Procedure).

Thermodynamic Calculations

The thermodynamic predictions of the chemical stability of various dispersoids in Be were based on calculating the Gibbs free energy of reaction (ΔG). The composite system was treated as a series of generic chemical reactions of the dispersoid and/or matrix with Be at a given temperature and composition, constrained by atom balances. The reaction having the lowest free energy (most negative ΔG of reaction) provided insight into the favored composition for that model system as well as the overall chemical stability of the composite.

The parameters for calculating the free energies of reactant and product species were obtained from a variety of sources: the assessed binary phase diagrams of Ti and Be (ASM International); Smithells Metals Reference Book; direct calculation using C_p , H , and S data; and the JANNAF Thermochemical Data Tables. The free energy, G , is calculated as a function of temperature (T) using enthalpy, entropy, and heat capacity data by

$$\Delta G(T) = (\Delta H_{298} + \int C_p dT) - T [\Delta S_{298} + \int (C_p/T) dT], \quad (1)$$

where

C_p = Heat capacity

H = Enthalpy

S = Entropy.

Terms were also included for phase changes. For intermetallic species and solutions, free energy data is found in the assessed phase diagram literature. G , for line compounds such as $TiBe_{12}$, is typically represented by

$$G(T) = A + B(T) \quad (2)$$

where A and B are constants.

For solutions or defect structures, G is calculated from solution thermodynamics,

$$G_{\text{ideal}} = \sum x_i G_i^{\circ} + RT \sum (x_i \ln x_i) \text{ and} \quad (3)$$

$$G_{\text{regular}} = G_{\text{ideal}} + G_{\text{excess}} \quad (4)$$

where

x_i = atomic fraction

G_i° =

R = gas constant

C = constant

D -- = constant

G_{excess} is generally of the form of Πx_i (constant) or $\Pi x_i (C + Dx_i)$, corresponding to regular and subregular solution models, respectively. For ternary solutions, pairwise additivity of the excess free-energy binary terms was assumed.

For a given combination of XD master alloy and Be, the system was treated as a set of chemical reactions and the free energies of reaction were calculated. For example, in the $\text{Ti}_5\text{Si}_5 + \text{Ni}$ -in-Be system, the following reaction products were used:

- 1) $\text{Ti}_5\text{Si}_3 + \text{NiBe}(\text{beta}) + \text{Be}$
- 2) $\text{Ti}_5\text{Si}_4 + \text{TiBe}_{12} + \text{NiBe}(\text{beta}) + \text{Be}$
- 3) $\text{TiSi} + \text{TiBe}_{12} + \text{NiBe}(\text{beta}) + \text{Be}$
- 4) $\text{TiSi}_2 + \text{TiBe}_{12} + \text{NiBe}(\text{beta}) + \text{Be}$
- 5) $\text{TiBe}_{12} + \text{NiBe}(\text{beta}) + \text{Si/Be}(\text{liq.})$
- 6) $\text{TiBe}_{12} + \text{Ni/Si/Be}(\text{liq.})$.

Other phases or reactions are conceivable -- eg., NiSi and NiSi₂. However, these particular phases have melting temperatures significantly below the anticipated casting temperature, and would therefore not be viable in the proposed process. Free energies lower than that of the reaction producing Product (5) above indicate the dispersoid is not stable in molten Be.

The atom balances for a 100-gram composite were performed to provide stoichiometric coefficients. The data references used in these calculations are listed in Table 1. The free energies of the reactions producing the above products were calculated at three temperatures and plotted (Fig. 2). The figure indicates that the dispersion of Ti₅Si₃ in NiBe(beta)+Be is not the preferred system -- TiBe₁₂ plus a Ni/Si/Be ternary solution is more stable. Ti₅Si₃ would not be expected to survive in molten Be. The reason for this lies in Be's reactivity and atom balance. Not only is Be highly reactive, but the large number of moles of Be drives the reduction or dissolution of the starting Ti-silicide.

Other candidate composites were similarly investigated. Silicides and oxides were the center of study. Earlier experiments and thermodynamic analyses showed that the introduction of TiC into Be results in the disproportionation of the carbide into Be₂C and TiBe₁₂. Borides were specifically excluded from this study due to concern of contaminating the test facility. The XD-based composites analyzed included:

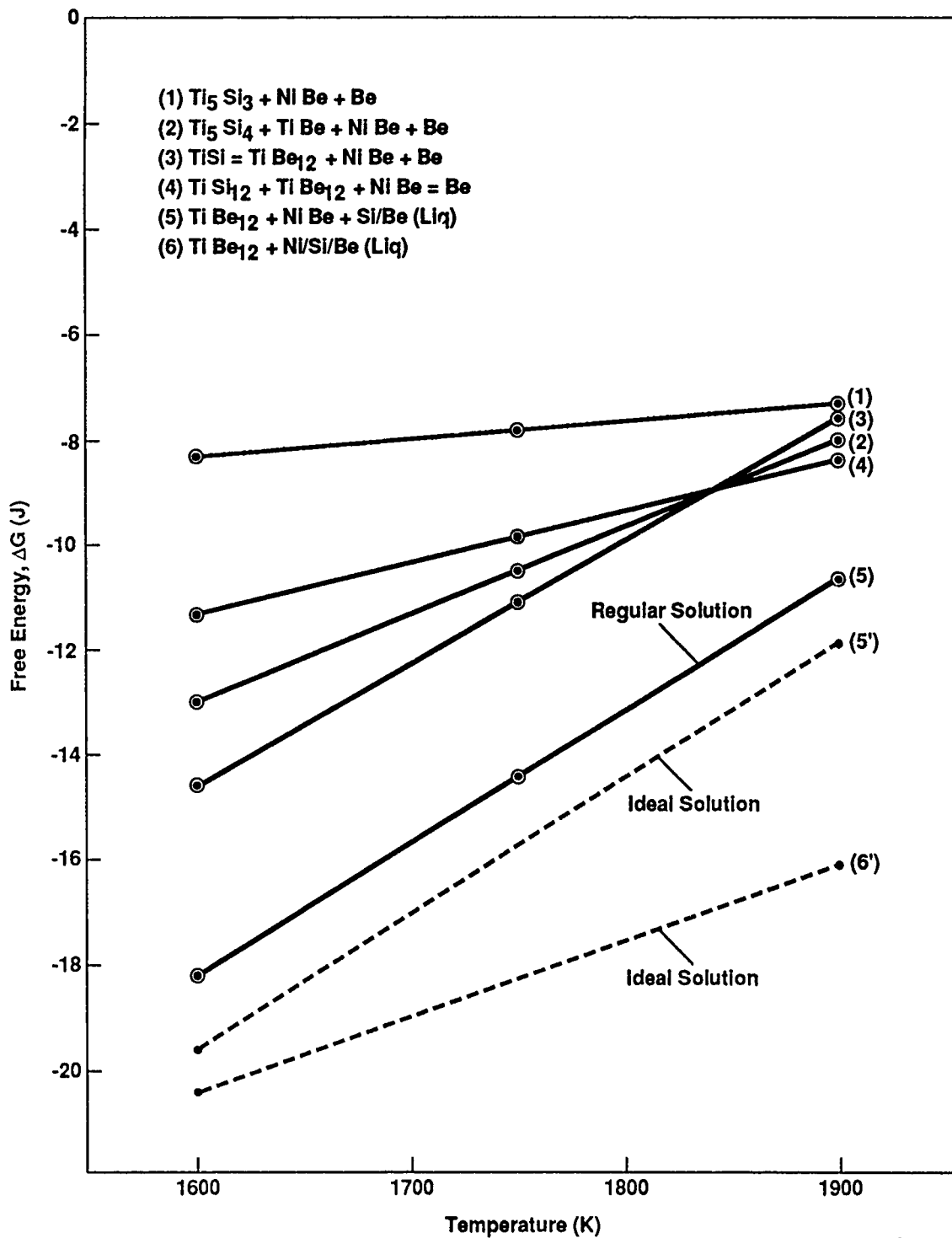
- o Ti₅Si₃ in Ni, Fe, and Ti
- o MoSi₂ in Cu
- o CoAl in Cu
- o Oxides (including TiO₂) in Cu
- o TiSi₂ in Ni.

No stable silicide, carbide, or oxide ceramic phase was identified. In all cases, both dispersoid and XD matrix materials reacted with or dissolved in the Be melt. The thermodynamic analyses were not extended to include precipitation upon cooling even through precipitates would be expected. While not chemically stable, some of these materials were synthesized and cast because they do offer a route to providing a stable phase with stable particles.

TABLE 1. Free Energies
for Stability Calculations.

Species	Reference
Ti ₅ Si ₃	4
Ti ₅ Si ₄	4
TiSi	4
TiSi ₂	4
TiBe ₁₂	5
Beta-NiBe	5
Binary solutions	Ideal- and real-solution thermodynamics G _{excess} - ASM-assessed phase diagrams
Ternary solutions	4,5

TO0456-1



T00090-1

Figure 2. Free energy as a function of temperature for chemical reactions between molten Be and an XD Ti_5Si_3 master alloy.

II. EXPERIMENTAL PROCEDURE

XD master alloys prepared at Martin Marietta Laboratories were melted and cast by Brush Wellman. Both Be and beta-NiBe matrices were studied. Various chemical families of particulates were tried in an attempt to produce a fine-grained dispersion. The fine stable dispersoids selected were Ti_5Si_3 , TiO_2 , and $MoSi_2$.

A complete list of master alloys is shown in Table 2. The master alloys were analyzed by X-ray diffraction (XRD) for phase identification and by scanning electron microscope (SEM) to see particle size and morphology.

All master alloys were made according to standard XD technology. Powders were weighed, blended for 1 hour in a ball mill, pressed to about 65 percent theoretical density, and reacted. The materials in Table 3 were used.

All concentrates were synthesized and analyzed at Martin Marietta, while castings, rolling operations, and the metallography of the products were done at Brush. The master alloys were either diluted in beryllium or combined with sufficient nickel to form the beta-NiBe.

The beryllium and beryllium intermetallic billets were cast using vacuum-cast beryllium lump and electrolytic nickel as input material. Starting materials were cleaned, degreased, placed in a BeO crucible, and induction-heated in a vacuum in the 10^{-3} torr range. The temperature of the melt was monitored using an optical pyrometer. All billets were held molten for 5 minutes, and were then cast with a $200^{\circ}C$ superheat into an unheated graphite mold.

The dispersoid-containing material was received from Martin Marietta Laboratories in the form of small billets. The billets were weighted, sectioned, and cleaned before casting. A 10-weight percent loading of dispersoid in the beryllium was selected for all castings. During the course of experimentation, excessive slagging and gas evolution was

TABLE 2. XD-Be Master Alloys List.

Specimen No. (Master Alloy)	Brush Billet No. (Casting)	Composition of Master Alloy (Weight Percent)	Composition of Casting
I. Be matrix			
None	Be-0	N/A	Pure Be
Be-1	Be-1	35% TiC/Cu	10% TiC/Cu w/Be matrix
Be-2	Be-2	33% Ti ₅ Si ₃ /Cu	10% Ti ₅ Si ₃ /Cu w/Be matrix
Be-3	Be-3	33% Ti ₅ Si ₃ /Ni	6% Ti ₅ Si ₃ /Ni w/Be matrix
Be-4	Be-5	33% Ti ₅ Si ₃ /Ti	10% Ti ₅ Si ₃ /Ti w/Be matrix
Be-5	Be-4	TiO ₂ /Cu (Stolch.)	10% TiO ₂ /Cu w/Be matrix
Be-6	Be-9	50% MoSi ₂ /Cu	10% MoSi ₂ /Cu w/Be matrix
Be-10*	None	65% MoSi ₂ /Cu	None
Be-12	Be-10	50% CoAl/Cu	10% CoAl/Cu w/Be matrix
II. Beta-NiBe matrix			
None	Be-6	N/A	Pure beta-NiBe
Be-7	Be-7	50% Ti ₅ Si ₃ /Cu	10% Ti ₅ Si ₃ /Cu w/beta-NiBe matrix
Be-8*	None	60% Ti ₅ Si ₃ /Cu	None
Be-9	Be-8	70% Ti ₅ Si ₃ /Ni	10% Ti ₅ Si ₃ /Ni w/beta-NiBe matrix
Be-11*	None	60% Ti ₅ Si ₃ /Ti	None

*Not cast

TO0456-2

TABLE 3. Master Alloy Materials.

Material	Purity	Size μm	Vendor
Al	99.5	-44-149	Consolidated Astronautics
C	99.9	2	Consolidated Astronautics
Co	99.8	-44	Consolidated Astronautics
Cu	99.5	-44	Consolidated Astronautics
Mo	99.9	5-10	Consolidated Astronautics
Ni	99.2	-44	Consolidated Astronautics
Si	99.8	-44	Consolidated Astronautics
Ti	99	10	Unifide

TO0456-3

observed when the dispersoid was added to the melt. A dewatering sequence was developed to remove residual moisture from the pores of the dispersoid billets. The billets were soaked in acetone, rinsed, resoaked, and then heated to 150°C for 12 hours. This operation greatly reduced slag formation.

Two methods were used to add the dispersoid to the melt. An initial attempt was made to load the billets into the melt through a load lock. A major problem with this method was melt chill and resolidification. The equipment design required that the charge be added to the melt cold. When the dispersoid billet was added to the melt, the heat capacity of the charge was large enough to cause local resolidification of the melt. In addition, an oxide skin, difficult to break during remelting, formed around the dispersoid-containing billet. Consistent results could therefore not be obtained using this method. Success was achieved by partially melting the beryllium and then placing the dispersoid billets on the surface of the unmelted charge. This allowed the dispersoid billet to preheat before it contacted the melt. When the remaining beryllium melted, the dispersoid material fell into the melt. This event was observed, and the billet was cast into the mold 5 minutes later.

Each cast billet was sectioned for metallographic and chemical analysis. For consistency, the specimens were taken from the same location in each billet. The sections were mounted, polished, and photographed. In addition, the chemical composition of the phases present in the samples was also identified using energy-dispersive X-ray analysis (EDXA). X-ray diffraction was also attempted, but the low-volume fraction of second-phase particles greatly reduced the effectiveness of this technique.

Thin slices were used for the analysis without texture correction. It is therefore possible that oriented phases were unobserved, but nothing was observed in the microstructure of specimens to indicate particle number orientation.

Rolling blocks, in the form of thin slices, were cut from each of the billets. The binary NiBe billet was easily sliced, but the NiBe material containing dispersoids cracked during cutting and rolled billets were not

produced. The rolling blocks were canned in steel and preheated for 1 hour. The canned blocks were then rolled using a schedule provided by Martin Marietta Laboratories. The sheets were decanned, photographed, and sectioned in the lateral (L) and transverse (T) directions. Further metallographic preparation and analysis was done by a method similar to that used for the cast material.

A. CASTING

Eleven billets were cast for this program; a beryllium control, seven beryllium billets containing different dispersoids or carriers, a NiBe control, and two NiBe dispersoid-containing billets. The billets and their contents are listed in Table 4.

Each billet weighed about 750 grams (1400 grams for the NiBe billets) and had dimensions of 5x15x8 cm. Macrographs of sections of billets Be-6 and Be-10 are shown in Fig. 3. External pipe, shrinkage, and gas porosity was observed in the billets. A large central pore can be observed in Be-10. The amount of shrink in the castings was a result of pouring into a cold mold. Both the pipe and shrink could be reduced by modifying the mold design and providing for directional heat removal.

B. CROSS-ROLLING

The rolling schedule used to produce the beryllium sheet samples is shown in Table 5. The schedule reproduces the schedule obtained from Martin Marietta Laboratories, but the thicknesses are actual mill gap values. Also note that the rolling packs were rotated 90 degrees three times during rolling.

Flat, crack-free sheet material was produced by cross-rolling. Photographs of the sheet are presented in Fig. 4. Only two samples cracked in pieces, although two others were severely cracked and rendered unusable for anything other than metallography. The specimens rolled and their status after rolling are listed in Table 6.

TABLE 4. Billet Designations, Dispersoids, and Carrier Materials.

Billet No.	Matrix	Dispersoid	Carrier
Be-0	Be	None	None
Be-1	Be	TiC	Cu
Be-2	Be	Ti ₅ Si ₃	Cu
Be-3	Be	Ti ₅ Si ₃	NI
Be-4	Be	TiO ₂	Cu
Be-5	Be	Ti ₅ Si ₃	Ti
Be-6	NIBe	None	None
Be-7	NIBe	Ti ₅ Si ₃	Cu
Be-8	NIBe	Ti ₅ Si ₃	NI
Be-9	Be	MoSi ₂	Cu
Be-10	Be	CoAl	Cu

A 10-percent dispersoid load was used for all but billet Be-3, which was 6 percent. All billets were cast with 200°C superheat into a chilled mold.

TO0456-4



Figure 3. Macrographs of as-cast billets Be-6 and Be-10, with large shrinkage pores in both castings.

TABLE 5. Rolling Schedule
for XD Beryllium Cross-Rolled Blocks.

Pass	Mill Setting	Pass Reduction (Percent)	Accumulated Reduction (Percent)	Temperature (°C)	Comments
1	0.975	2.5	2.5	1038	Seating pass
2	0.840	13.8	16.0	1038	
3	0.707	15.9	29.3	1038	
4	0.600	15.1	40.0	982	1/4 turn
5	0.507	15.5	49.3	982	
6	0.427	15.8	57.3	982	
7	0.333	21.9	66.7	871	1/4 turn
8	0.267	20.0	73.3	871	
9	0.213	20.0	78.7	816	1/4 turn
10	0.173	18.8	82.7	760	
11	0.133	23.1	86.7	760	
12	0.113	15.0	88.7	760	

Initial rolling block thickness was 0.5 inch.

TO0456-5

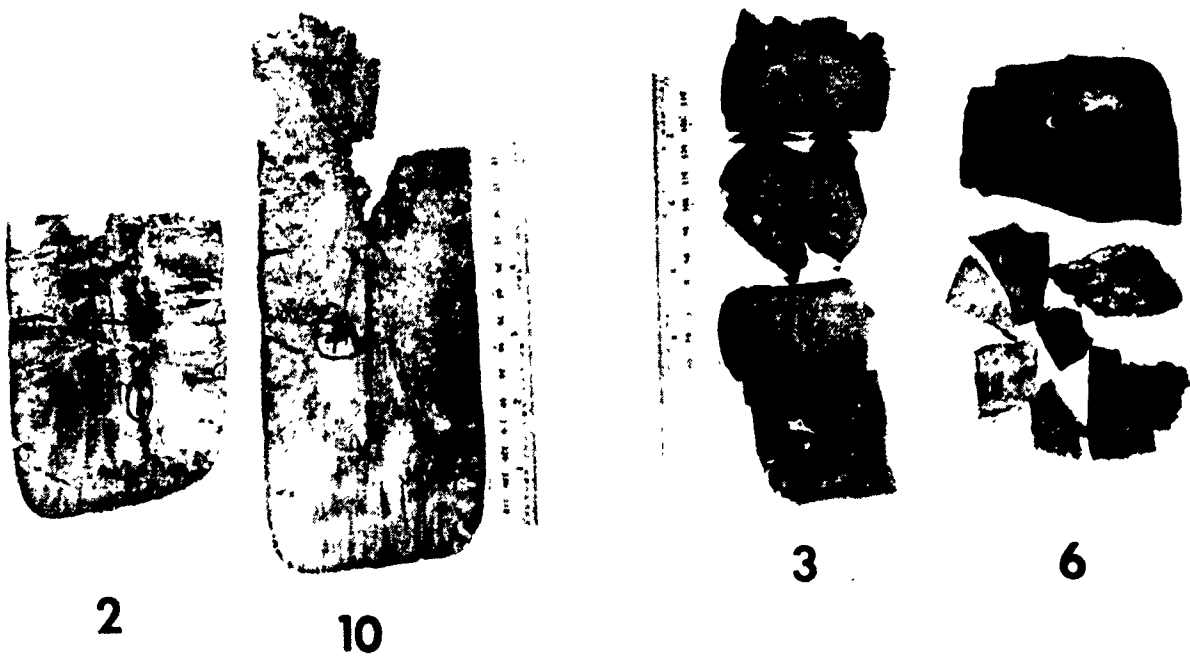
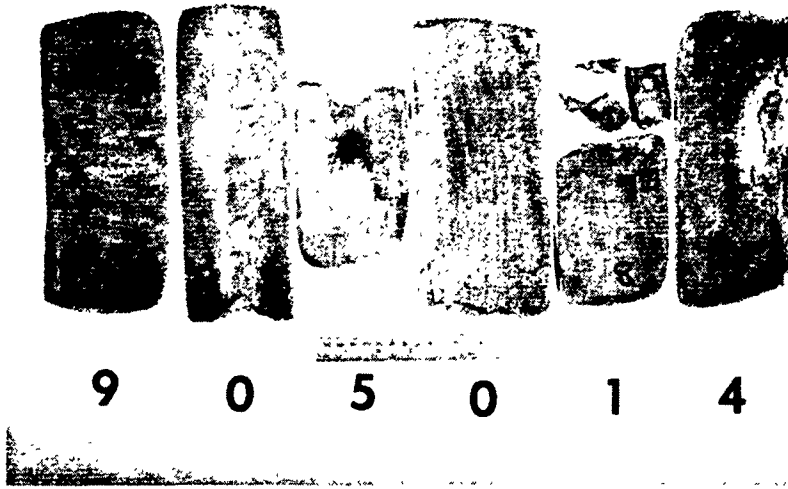


Figure 4. Macrographs of rolled billets with billet numbers below each billet and pack numbers indicated on several of the sheets.

Table 6, Rolled Specimen Inventory and Status.

Billet No.	Matrix / Dispersoid	Thickness (in.)	Comments
Be-0	Be/none	0.095	OK
Be-1	Be/TiC	0.098	Duplicate with large pore
Be-2	Be/Ti ₅ Si ₃	0.096	Center crack, delamination
Be-3	Be/Ti ₅ Si ₃	0.092	Severly Cracked
Be-4	Be/TiO ₂	0.104	Broke up during Rolling
Be-5	Be/Ti ₅ Si ₃	0.095	OK
Be-6	Be/Ti ₅ Si ₃	0.104	OK, some delamination
Be-7	NiBe/none	0.126	Cracked on rolling
Be-8	NiBe/Ti ₅ Si ₃	-	
Be-9	NiBe/Ti ₅ Si ₃	-	
Be-10	Be/MoSi ₂	0.103	OK, rolled well
	Be/CoAl	0.108	Cracked and delaminated

Table 7, Tensile Test Results:

Specimen	Offset Yield (0.2%)	UTS (Ksi)	Elongation %	Test Temperature	Elasticity Modules
Be-0	41.4	49.4	2.1	Ambient	38.3
Be-4	35.9	40.9	1.6	Ambient	41.7
Be-5	na	na	-	Ambient	Defective Test sample
Be-9	na	na	-	Ambient	Defective Test Sample

Centerline delamination and cracking were observed in several specimens. Specimens exhibiting this behavior had a large crack or series of cracks parallel to the faces of the sheet. Some specimens exhibited cracks that ran along grain boundaries in the original casting. It appears that the grain boundaries are not strong enough to withstand the rolling load and therefore fracture.

C. MICROSTRUCTURE

The X-D master alloy billets, both in the as-cast form and after mechanical working, were examined metallurgically. X-ray diffraction analyses were also performed on selected specimens throughout the program.

D. POLE FIGURES

The data necessary to construct the pole figures for selected specimens were obtained using chromium K-alpha radiation and a stepper-motor-driven Schulz back-reflection pole figure device, mounted on an automated Bragg-Brentano focusing geometry horizontal X-ray diffractometer.

The diffracted intensity data were collected for 1.0 second at each point (spaced at approximately 2 degrees in all directions) on a nominally equal area spherical net throughout the central 80 degrees of the pole figure.

During data collection, the sample was oscillated +/- 0.5 cm in a plane parallel to the sample surface, in order to integrate the diffracted intensity over the maximum sample surface possible.

The background intensity measured on both sides of the diffraction peak for each angle of tilt was interpolated to determine the background intensity component of the diffraction peak. After subtraction of the background, the corrected pole figure was constructed in spherical coordinates by linear interpolation of the data collected on the equal area spherical net.

The data were then used to create stereographic projection pole figure plots. Because a random sample was provided for reference, a true times-random pole figure was produced in accordance with ASTM Specification E81. The times-random data were also corrected for defocusing intensity losses as a function of the angle of tilt. The times-random pole figure is presented as a log scale contour plot to allow observation of details.

E. MECHANICAL TESTING

Selected specimens as presented in Table 7 were tensile tested. The specimens were prepared from as-rolled, stress relieved material. The micro tensile bars were 0.120 inch by 0.090 inch by 3.4 inch with gage lengths of 0.50 inch.

III. RESULTS AND DISCUSSION

Each of the systems studied are presented in terms of 1) predictions based on thermodynamic considerations; 2) what was observed for each XD master alloy; 3) what was observed for the alloy billets; and 4) what was observed from the rolling studies.

Note that, in some cases, the number of the casting differs from the number of the master alloy. Table 2 (Section II) correlates the two numbering systems.

A. CASTING Be-O: BERYLLIUM CONTROL SAMPLE

Micrographs of the cast structure of the pure Be billet are presented in Fig. 5. Note the absence of detail in the bright-field micrograph. The micrograph taken with polarized light shows the grain structure of the casting. Second-phase particles were not observed, although a few small pores were present in the microstructure. The twins evident in the grains are due to specimen preparation. The grains in the casting were columnar, and a meaningful grain size could not be determined. Rolling produced an equiaxed grain structure in the cast material, with little apparent elongation of the grains. Micrographs are shown in Fig. 6. Fig. 7 is the 002 pole figure which indicates some degree of texturing. The grain size of the rolled material was determined to be 160 micrometers. This can be compared to the grain size of a consolidated powder product, which ranges between 5 and 20 micrometers, and a rolled powder product, which ranges from 5 to 20 micrometers.

B. CASTING Be-1: 10-WEIGHT-PERCENT TiC IN Cu WITH A Be MATRIX

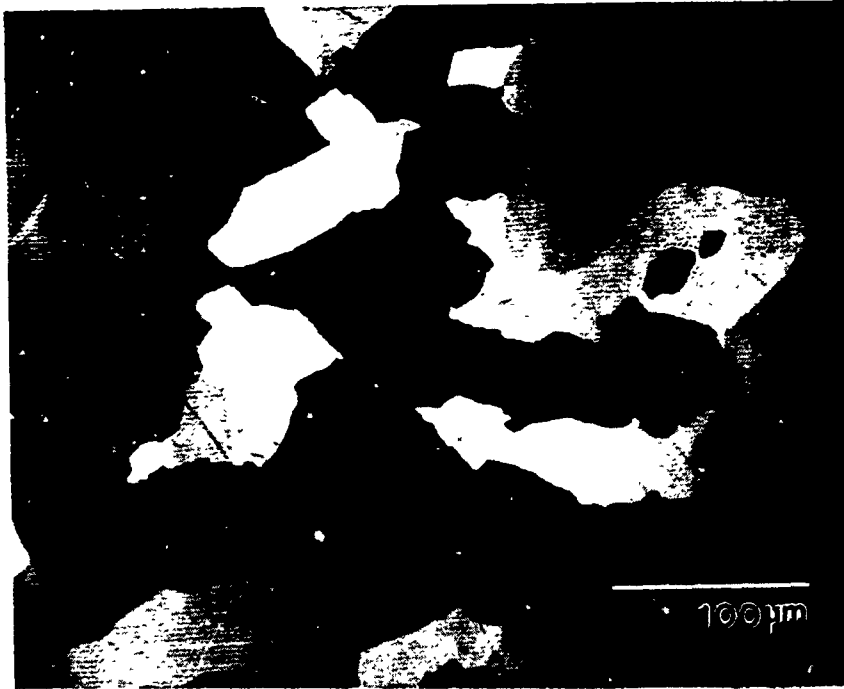
Predictions: Earlier studies and thermodynamic predictions showed that TiC would react with Be to form Be_2C and TiBe_{12} . Nonetheless, Be_2C and TiBe_{12} are both stable in Be and would be expected to survive melt processing.



Be-O

POL

Figure 5. As-cast Be-O.



Rolled Be-0

POL

L-direction



Rolled Be-0

POL

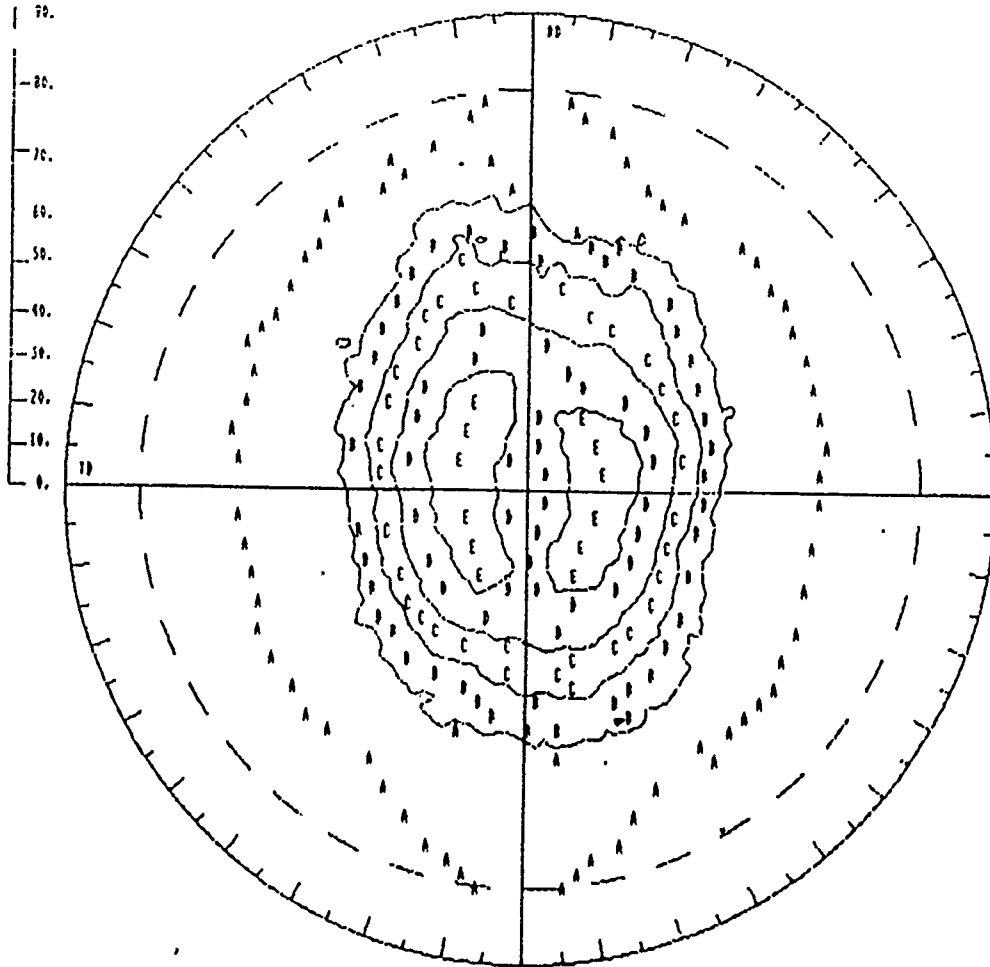
T-direction

Figure 6. Cross-rolled Be-0.

Figure 7

(002) Pole Figure
Stereographic Projection Plot. Times Random Format

Spec. Be-0 Kimm/.5NSPPole



Sym. x RANDOM

A (.00 - .24)

B (.25 - .49)

C (.50 - 1.00)

Sym. x RANDOM

D (1.01 - 2.00)

E (2.01 - 4.00)

2-Theta = 78.94 deg. Maximum intensity = 2097 Normal intensity = 397
Lambda = 2.29092 Angstroms Background 1 = 77.00 deg. Background 2 = 80.50 deg.

Maximum Times Random = 3.08

The XD Master Alloy: Master alloy Be-1 (35-weight-percent TiC/C) reacted as predicted to TiC + Cu. Particle size was estimated by SEM to be less than 1 micrometer (Fig. 8). XRD was clean and showed TiC and Cu.

The Alloy Billet: Microstructural examination of the casting revealed many small particles, 10 to 20 micrometers in diameter, in a large-grained beryllium matrix (Fig. 9a). Cracks were also observed in the microstructure. The grain morphology was columnar.

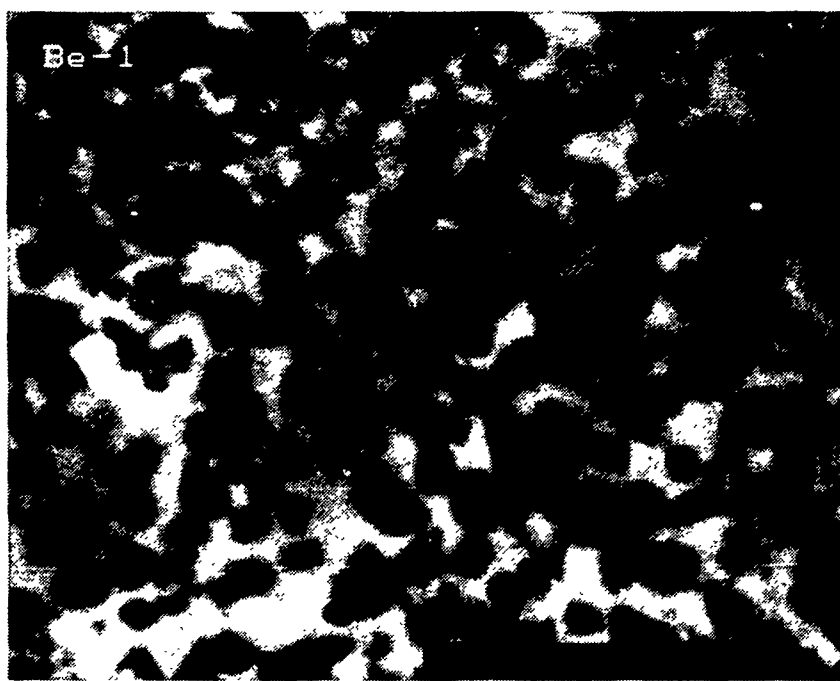
Numerous angular particles, uniformly distributed, were observed in the matrix (Fig. 9b). X-ray analysis of the particles did not detect the presence of any elements other than a trace of Cu and Ti (Fig. 10). On the basis of shape and X-ray data, these particles were identified as Be₂C.

Large dendritic particles, as well as colonies of another phase, were also observed in the microstructure. The colonies were regions of fine rods emanating from the larger particles. X-ray analysis showed that both the large phase and the rods were rich in Ti. Elemental X-ray maps for Ti and Cu taken in the SEM are shown in Fig. 11. Note that the Cu is uniformly dispersed, while the Ti is located in the particles. This is because Cu is very soluble in Be but Ti forms an intermetallic, TiBe₁₂, with Be. It appears that the TiC reacted with the Be to form Be₂C and one or more Ti-Be intermetallics.

Rolling Studies: Cross-rolling produced a refined grain size, as well as an elongated structure in the direction of rolling (Fig. 12). The grain size of the rolled material was 90 micrometers in the T direction. It appears that the dispersion of intermetallic particles has produced some refinement of the grain size.

C. CASTING Be-2: 10-WEIGHT-PERCENT Ti₅Si₃ in Cu WITH A Be MATRIX

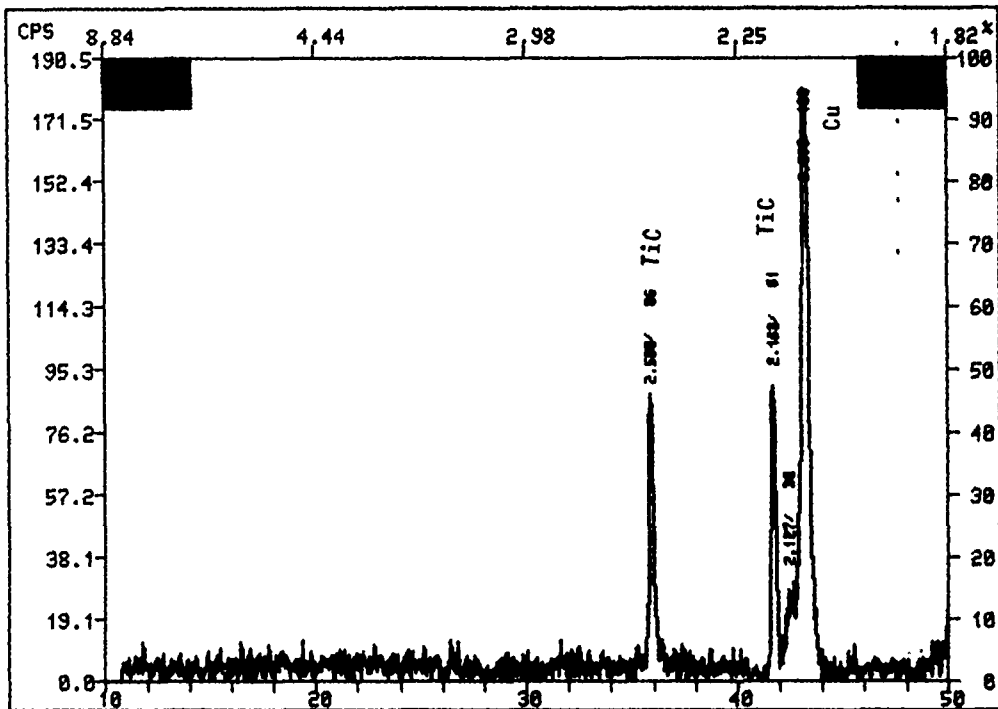
Predictions: Ti₅Si₃ was modeled extensively, and it was determined that although silicon is neither soluble in Be nor forms intermetallics, Ti₅Si₃ will dissolve in Be and/or form lower



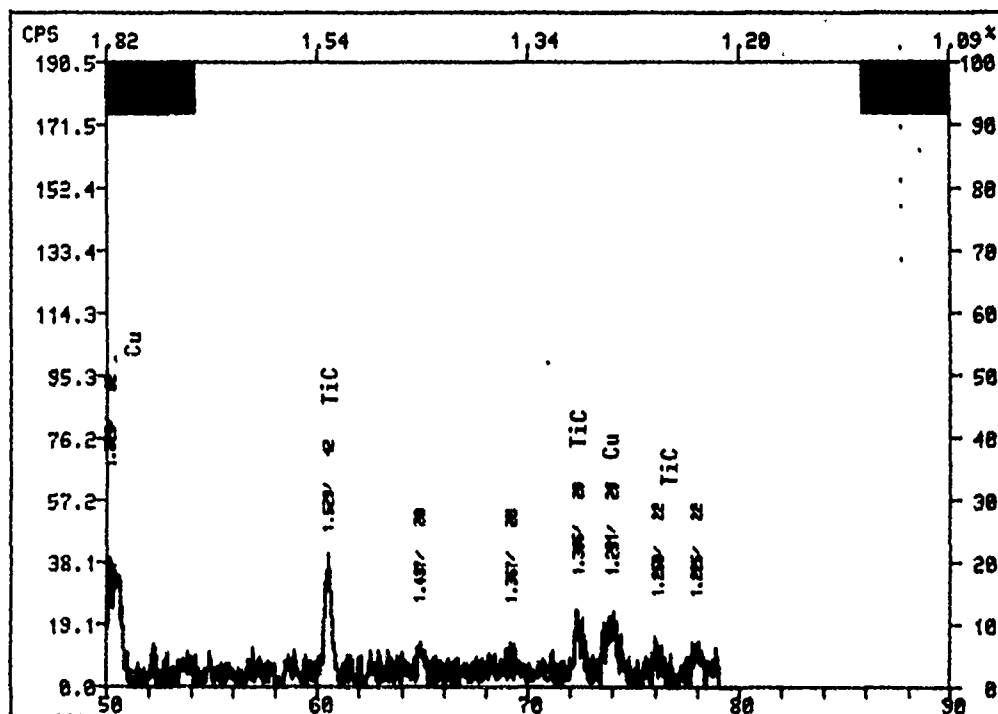
10 KX

a)

Figure 8. Scanning electron micrograph (a) and x-ray diffraction pattern (b1 and b2) of a TiC + Cu (35-weight-percent) master alloy (Be-1), 10,000X.



b1)



b2)

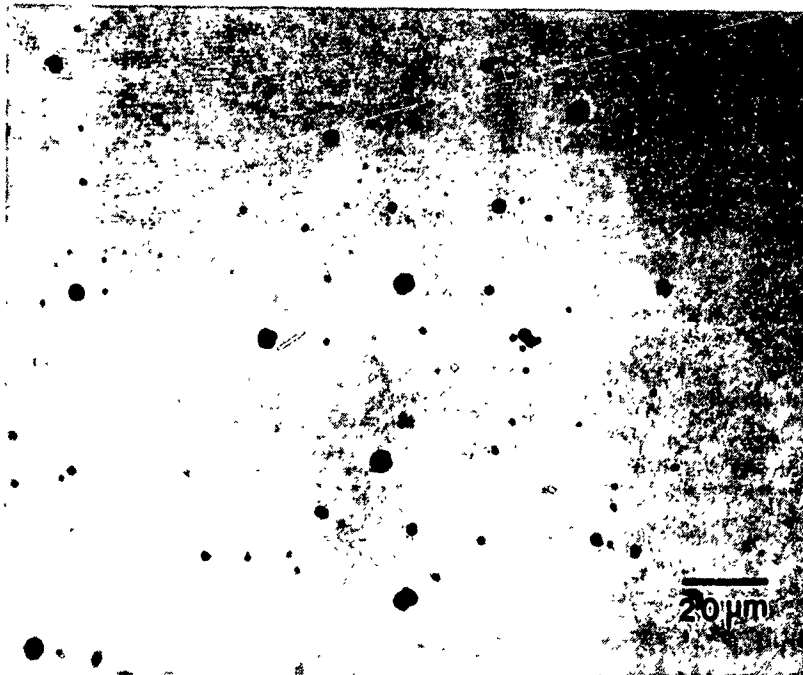
Figure 8. (Continued).



a.

Be-1

POL



b.

Be-1

BF

Figure 9. As-cast Be-1: 10-weight-percent TiC in Cu with a Be matrix.

BE TIC BILLET 3, DARK AREA, SPOT

SPECTRUM LABEL

1258 151V25M4, SPOT-53001, DARK ARE

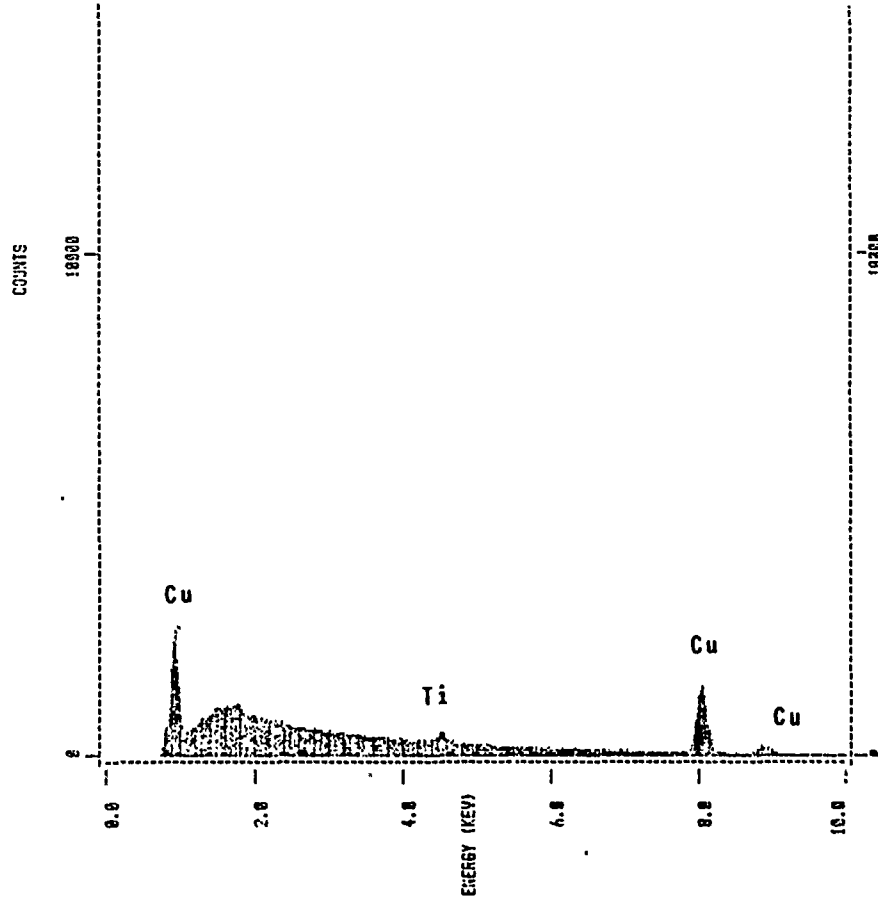
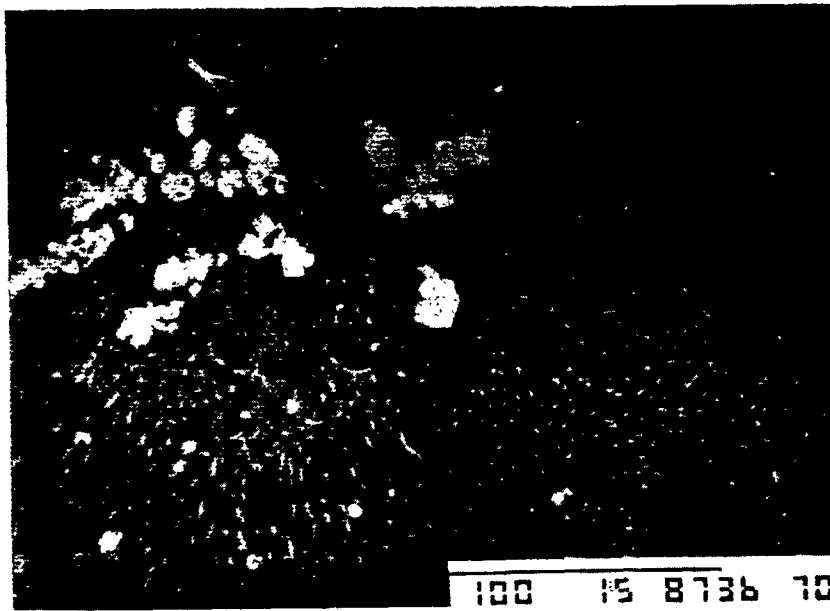
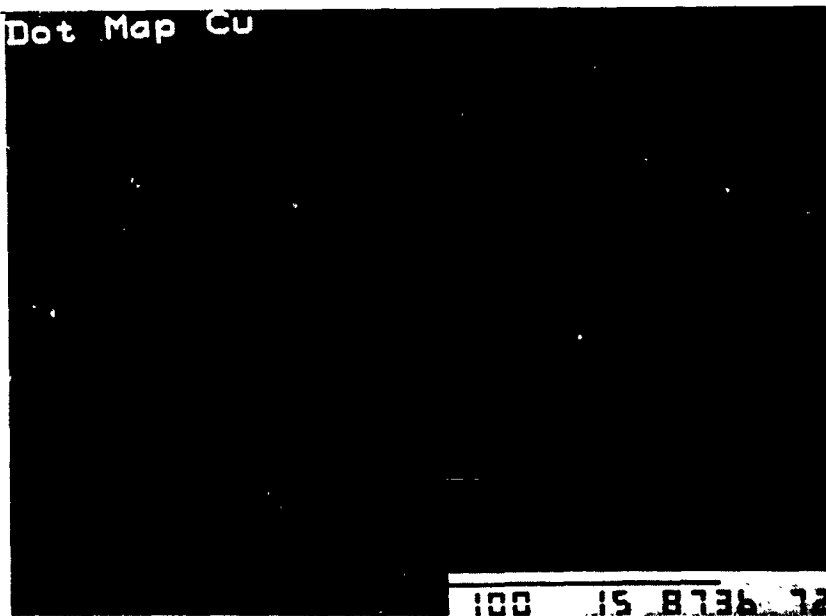


Figure 10. Spectra from angular particles (identified as Be₂C) in as-cast Be-1, with Cu and Ti resulting from the matrix.



Dot Map Cu



Dot Map Ti

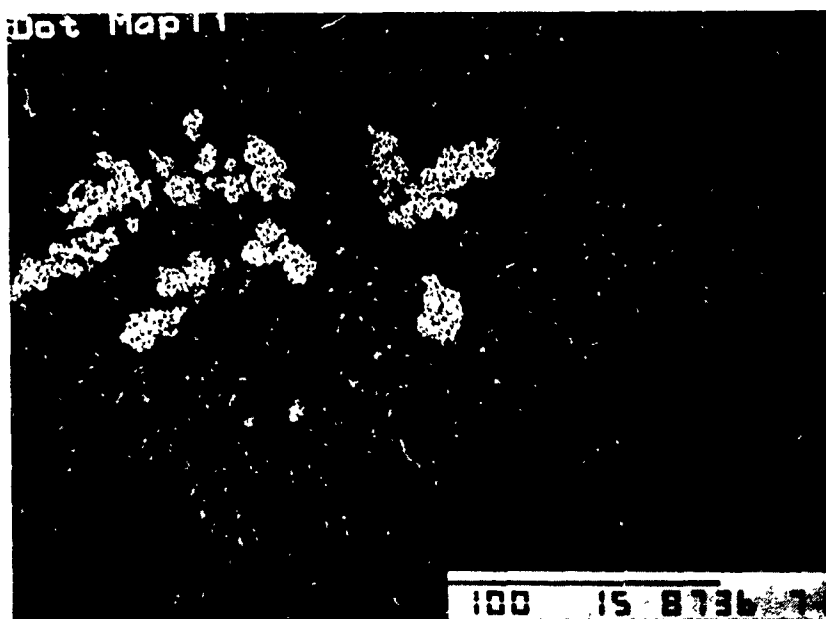
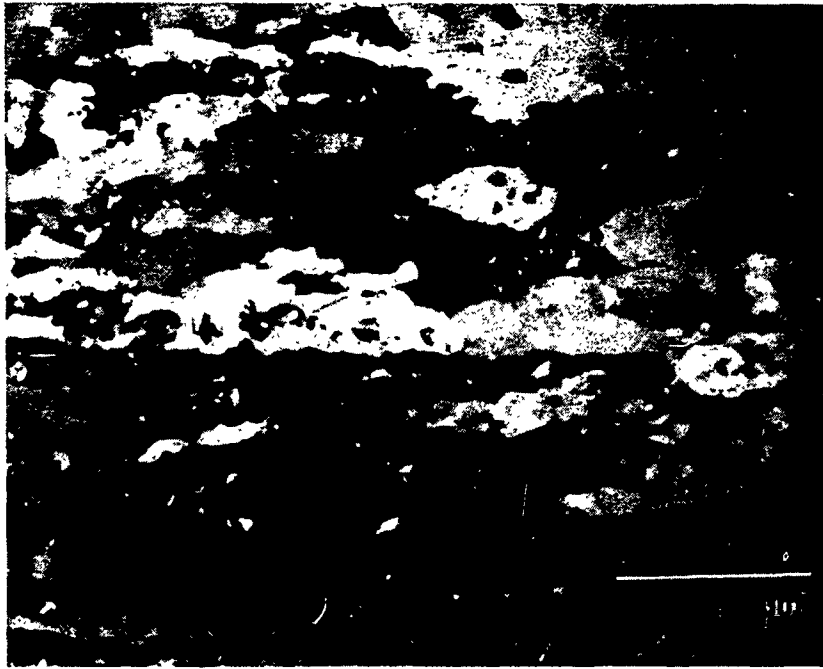


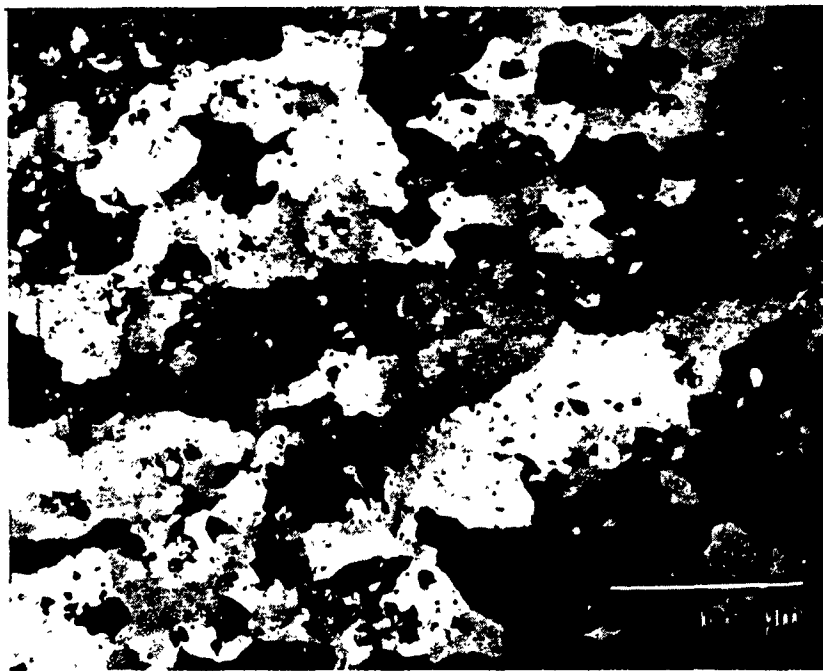
Figure 11. SEM micrographs of the Ti-rich phase in Be-1.



Rolled Be-1

POL

L-direction



Rolled Be-1

POL

T-direction

Figure 12. Microstructure of cross-rolled Be-1 sheet.

silicides, $TiBe_x$, and a Be/Siliquid solution. Upon solidification, the Si is expected to precipitate, possibly providing a dispersed phase. In a copper matrix, Ti_5Si_3 could be reduced by Be.

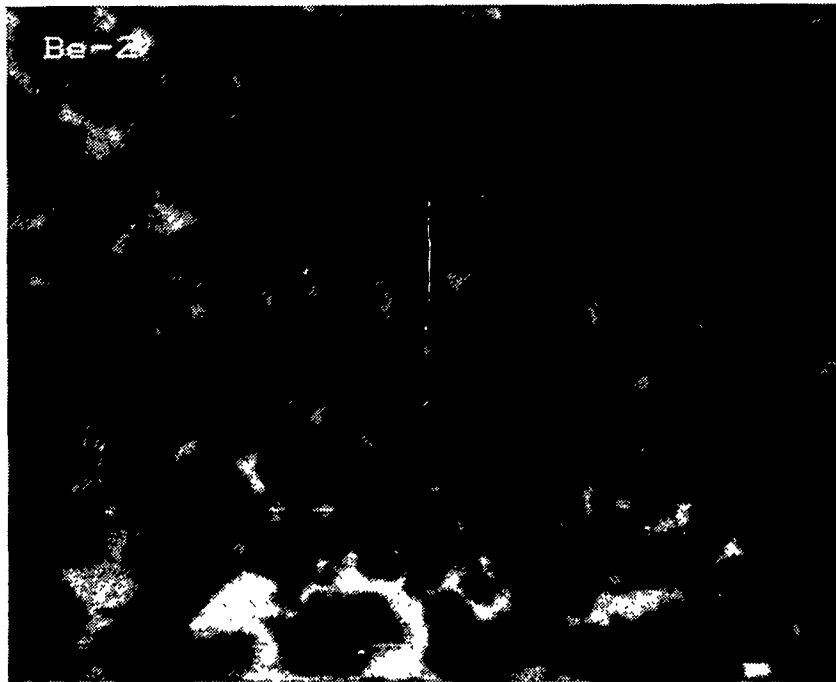
The X-D Master Alloy: Master alloy Be-2 (33-weight-percent Ti_5Si_3/C) also reacted was predicted. Particle size was 1 micrometer maximum; some particles appear to be very small (Fig. 13). The XRD showed only the target peaks.

The Alloy Billet: The microstructure of casting Be-2 and all castings that used Ti_5Si_3 as a dispersoid are similar. A large, blocky Ti-Be intermetallic was uniformly distributed throughout a large, columnar-grained Be matrix (Fig. 14a). Small regions of a phase identified as Si were located at grain boundaries and at isolated locations within the grains (Fig. 14b). Presumably, the Si results from the decomposition of Ti_5Si_3 by the Be matrix into a Ti beryllide and elemental Si. Due to the presence of a low-melting-point Be-Si eutectic, the Si is distributed in isolated pockets in the last-to-solidify regions.

X-ray dot maps of Ti, Si, and Cu obtained from a sample of the cast material are shown in Fig. 15. An X-ray spectrum obtained from one of the larger particles is shown in Fig. 16. Cu is present in the Be, and appreciable Si is present with the Ti. X-ray diffraction analysis of a slice of this sample indicated the presence of Be and $TiBe_{12}$. From the data, it appears that some Si segregated to the beryllide.

Small amounts of Be_2C were also observed in the matrix. The volume fraction of the phase was not as great as in Be-1, but some C did contaminate the melt.

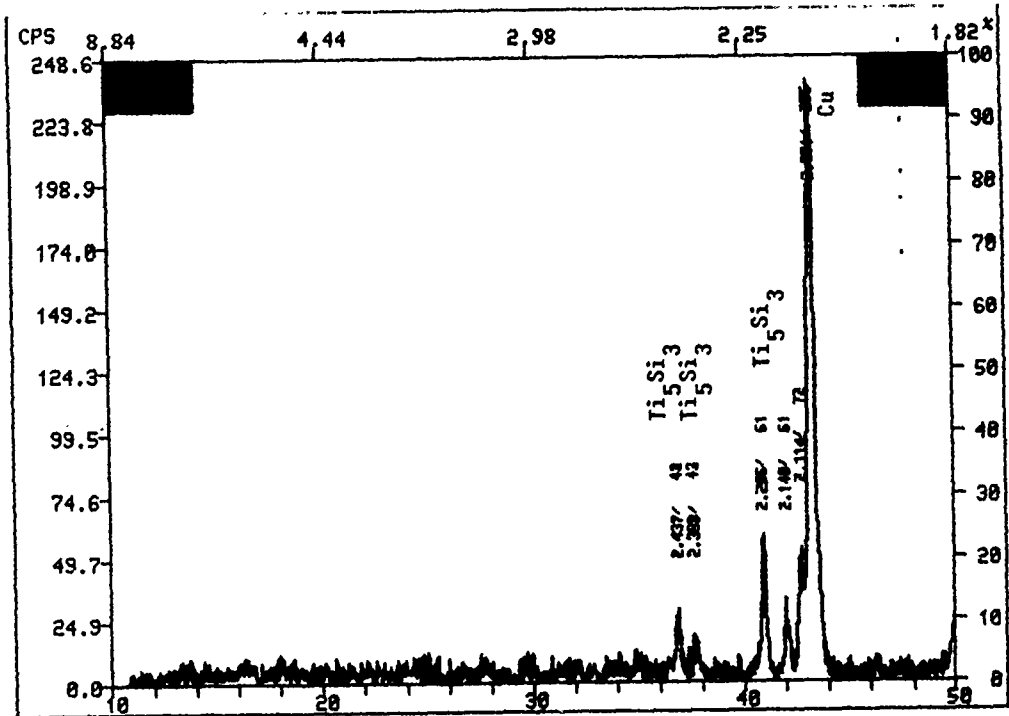
The microstructure of the cross-rolled sheet is presented in Fig. 17. The beryllides have formed long stringers in the sheet and have cracked and separated from the matrix (Fig. 18). Si-rich regions were observed adjacent to the Ti-rich particles. These remain from the original cast structure, although some Si may result from further decomposition of the Ti-rich particles to $TiBe_{12}$ and Si during the cross-rolling process.



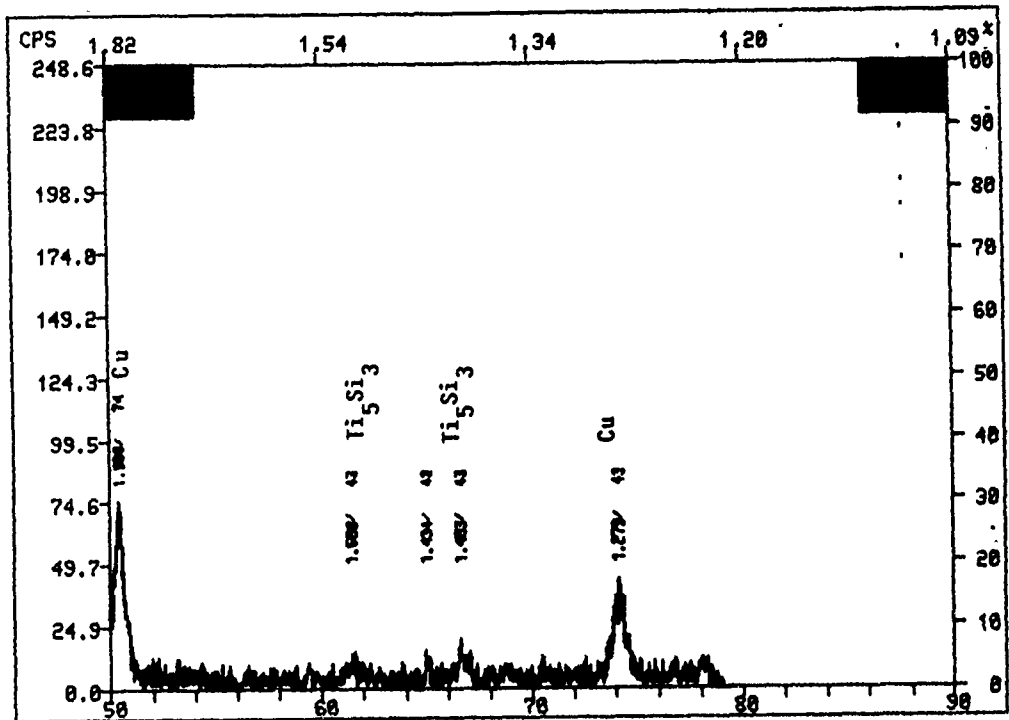
10KX

a)

Figure 13. Scanning electron micrograph (a) and x-ray diffraction pattern (b1 and b2) of a $Ti_5Si_3 + Cu$ (33-weight-percent) master alloy (Be-2), 10,000X.

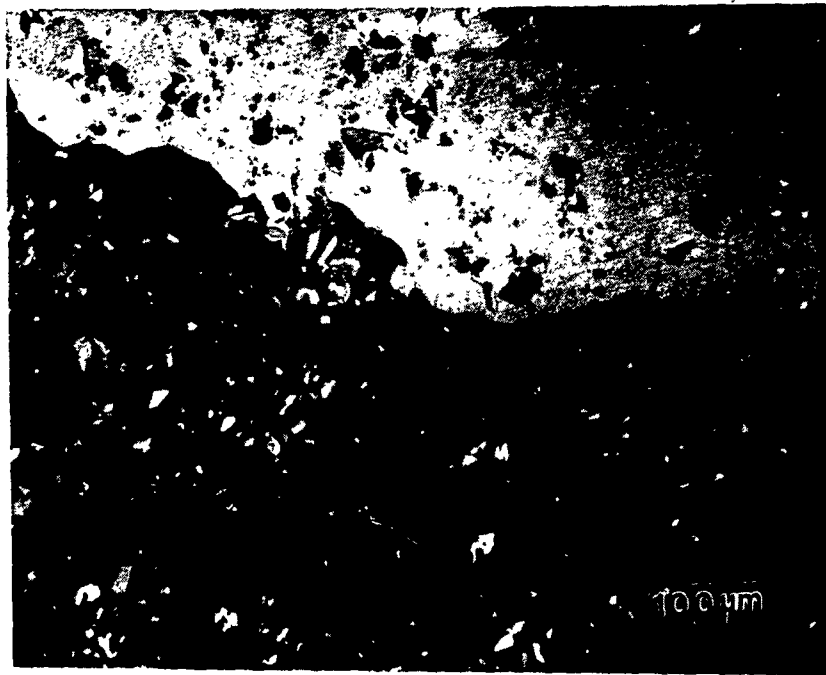


b1)



b2)

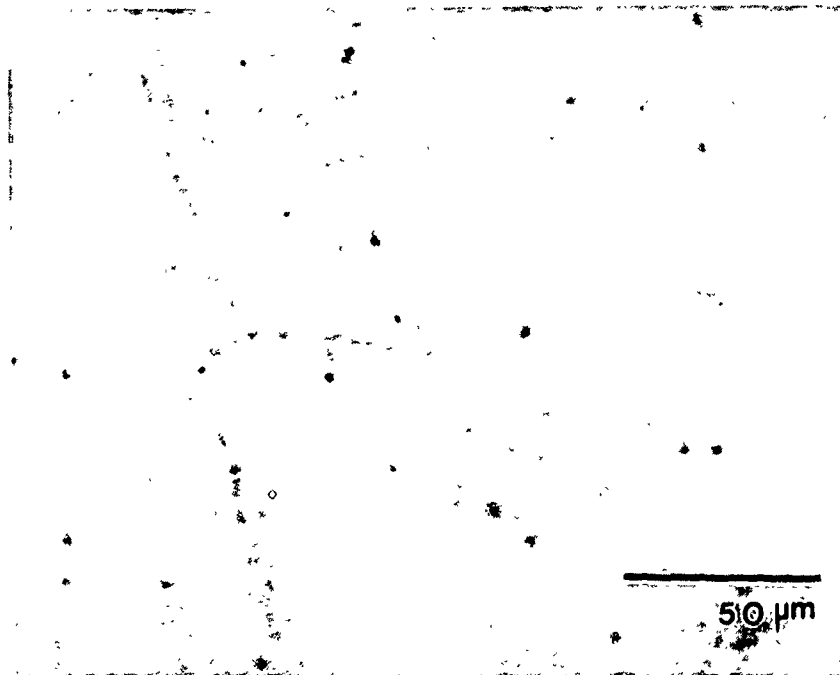
Figure 13. (Continued).



a.

Be-2

POL



b.

Be-2

BF

Figure 14. As-cast Be-2: 10-weight-percent Ti_5Si_3 in Cu with a Be matrix.

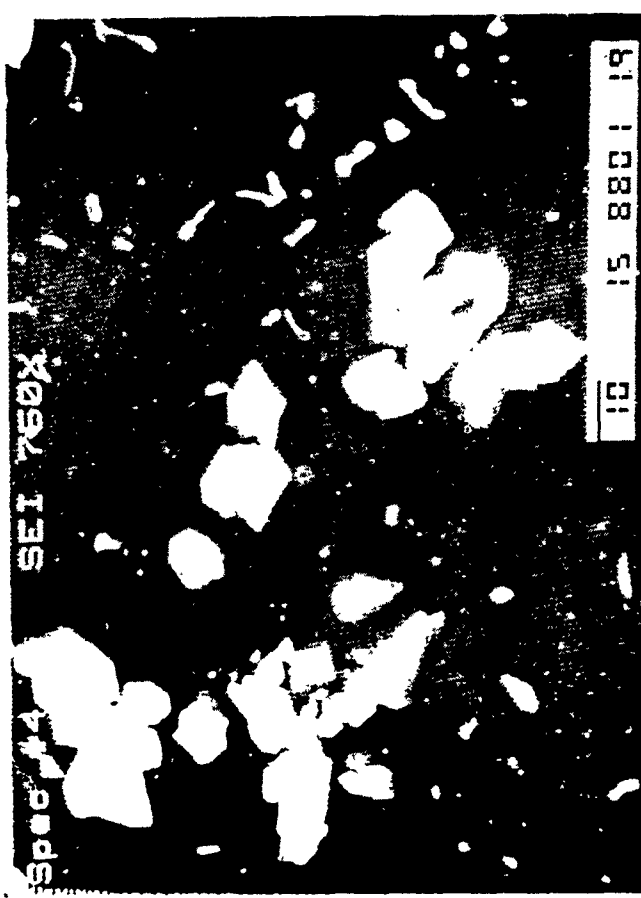
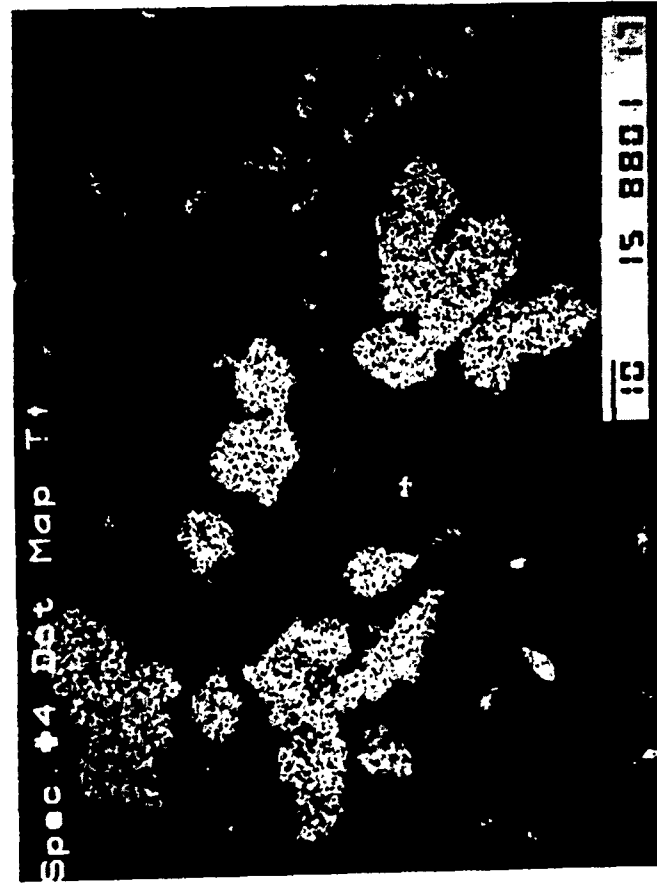
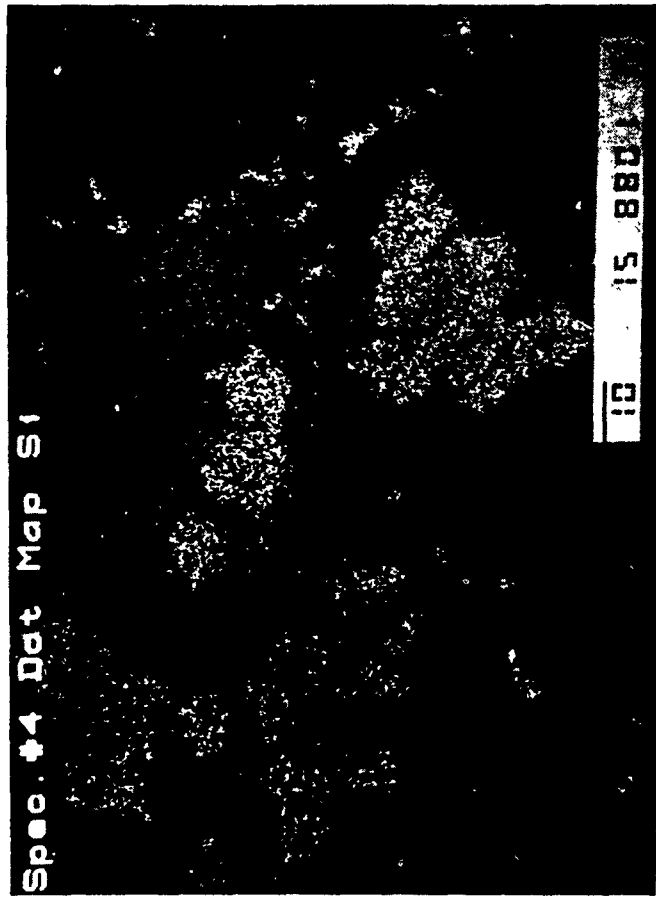
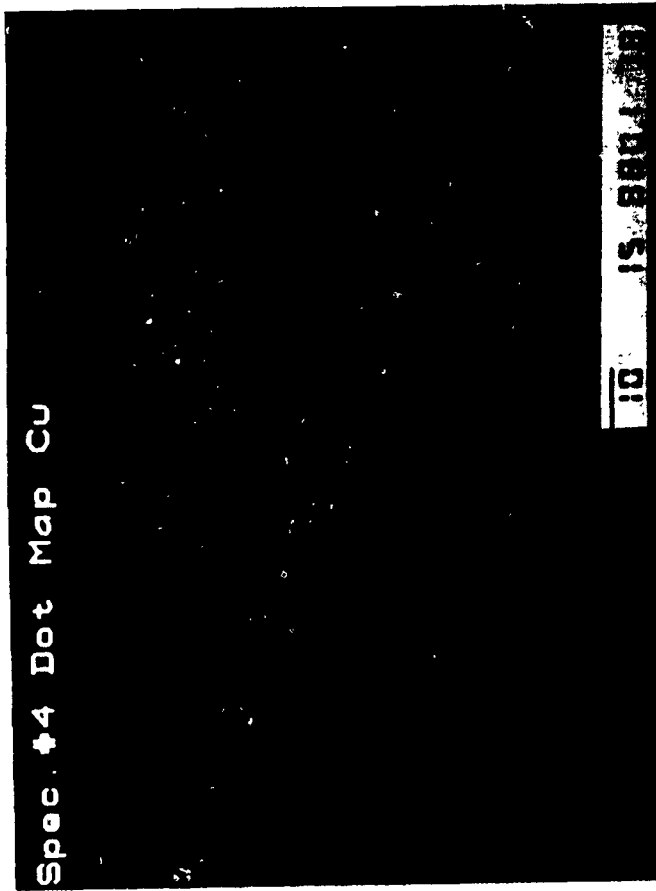


Figure 15. X-ray dot maps from the Ti-rich phase in casting Be-2.

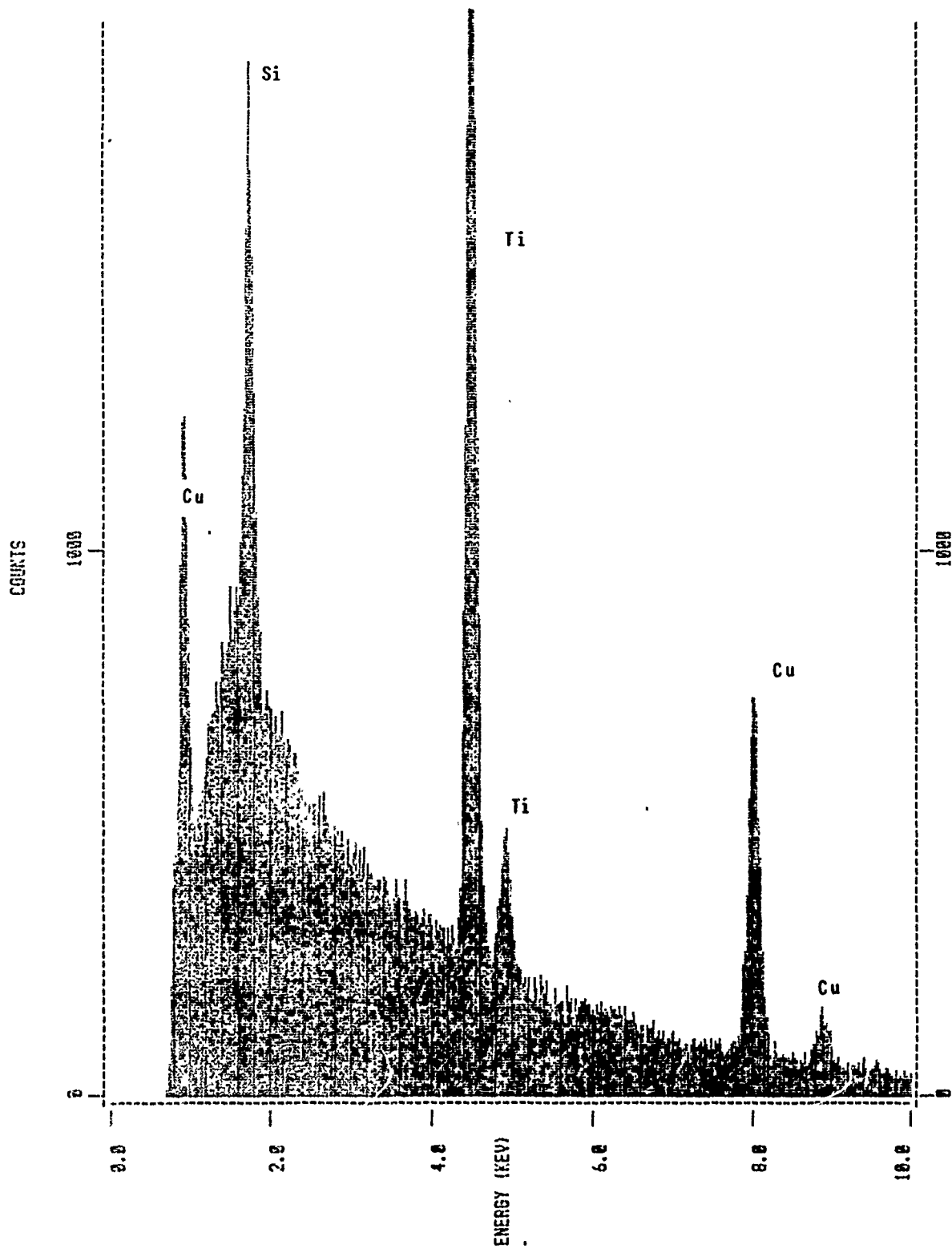


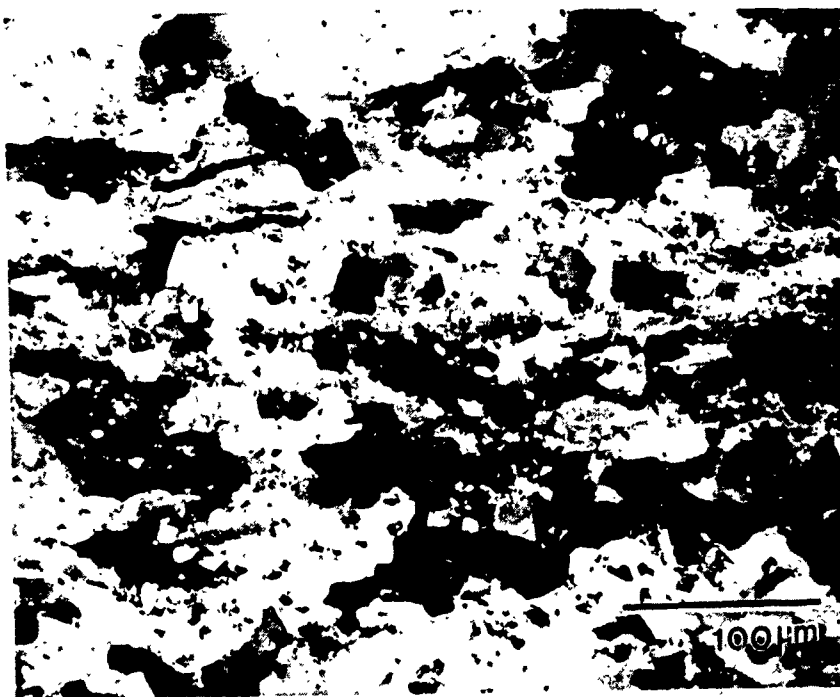
Figure 16. X-ray spectra of particles in billet Be-2.



Rolled Be-2

POL

L-direction



Rolled Be-2

POL

T-direction

Figure 17. Microstructure of cross-rolled Be-2.

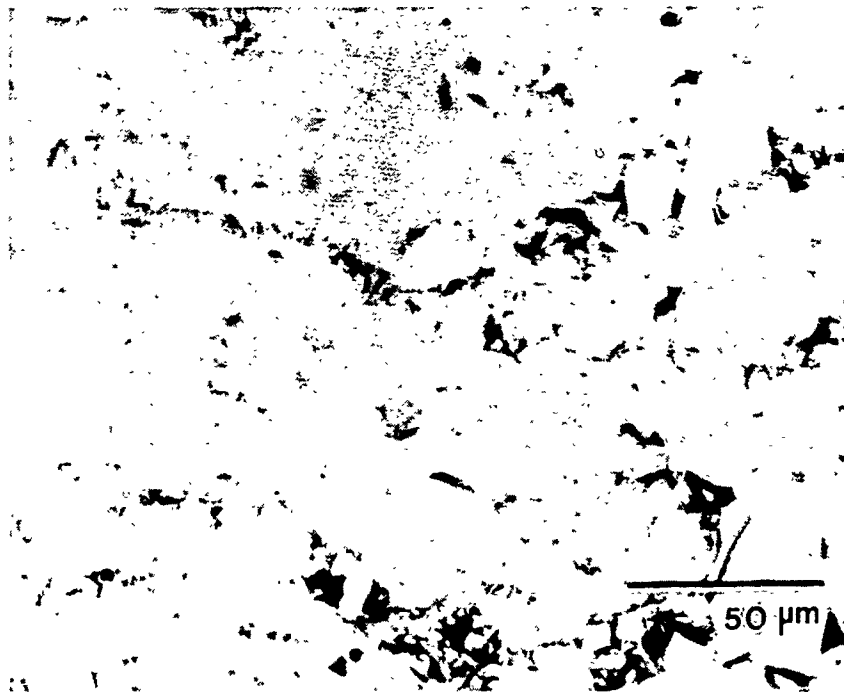


Figure 18. Si regions and cracked Ti-rich particles in Be-2 sheet.

D. CASTING Be-3: 6-WEIGHT-PERCENT Ti_5Si_3 IN Ni WITH A Be MATRIX

Prediction: Predictions for casting Be-2 apply equally to this casting. Additionally, Ti_5Si_3 would be reduced by Be but Ni in the master alloy would permit the Be to react, forming a Ni-beryllide that might stabilize the system.

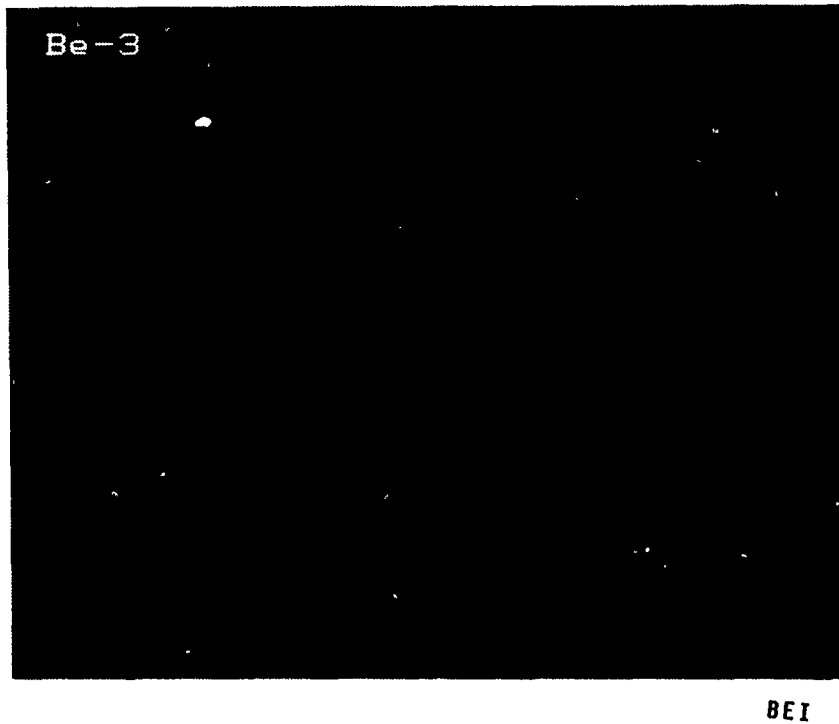
XD Master Alloy: Master alloy Be-3 (33-weight-percent Ti_5Si_3/Ni) reacted energetically, causing the matrix to partially melt and the reacted mass to flow. In this system, the particle size is basically meaningless. SEM shows more or less two continuous phases as opposed to the discrete particles in a continuous matrix normally seen from XD synthesis. XRD showed large amounts of a $Ni_{16}Ti_6Si_7$ phase (Fig. 19).

Alloy Billet: Micrographs of casting Be-3 are presented in Fig. 20. Large, blocky Ti-Be intermetallic particles were uniformly distributed throughout a large, columnar-grained Be matrix. Small interdendritic Si particles were also observed, as was Be_2C .

Rolling Studies: The microstructure of the cross-rolled sheet is shown in Fig. 21. The rolling operation did produce a refined grain size, but the intermetallic particles formed stringers. The microstructure of casting Be-3 in the cast and rolled condition was very similar to casting Be-2.

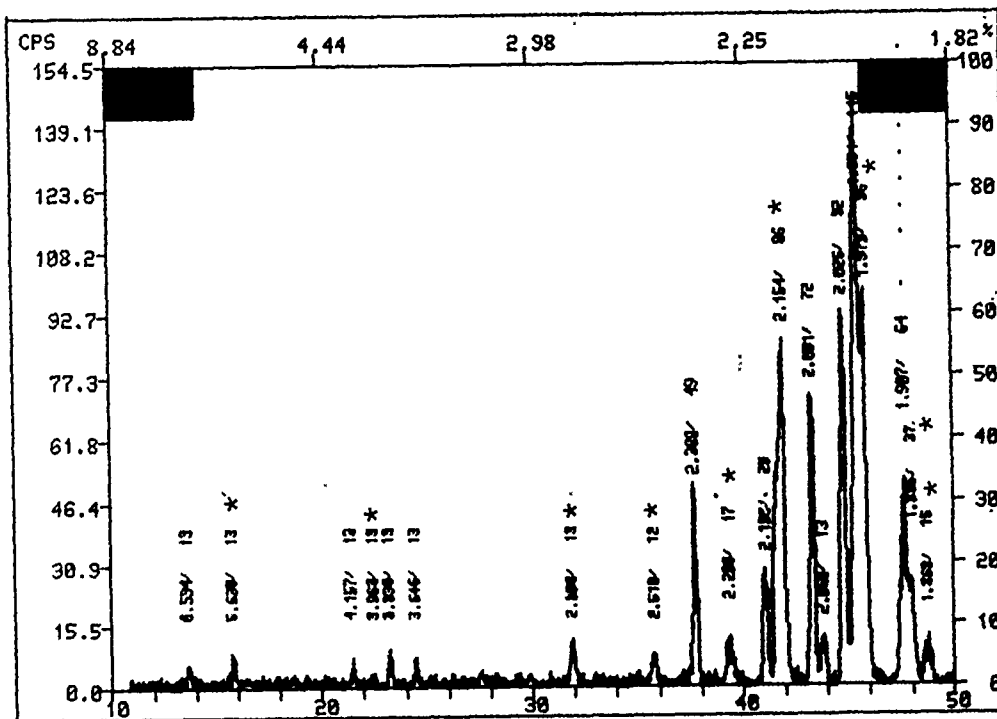
E. CASTING Be-4: 10-WEIGHT-PERCENT TiO_2 WITH A Be MATRIX

Predictions: Because metal oxides typically are either not wet by metals or their oxygen dissolves in metals of interest, oxides have not been synthesized by XD. However, BeO is extremely stable thermodynamically and will extract oxygen from most elements except for the rare earths and Ca. Moreover, oxygen does not dissolve in Be and prevents grain growth, as exploited in Be powder processing. If a metal oxide were synthesized and added to molten Be, the disproportionation reaction to BeO and the metal beryllide might provide the vehicle to obtain stable particles and grain refinement in Be, analogous to the carbide system.

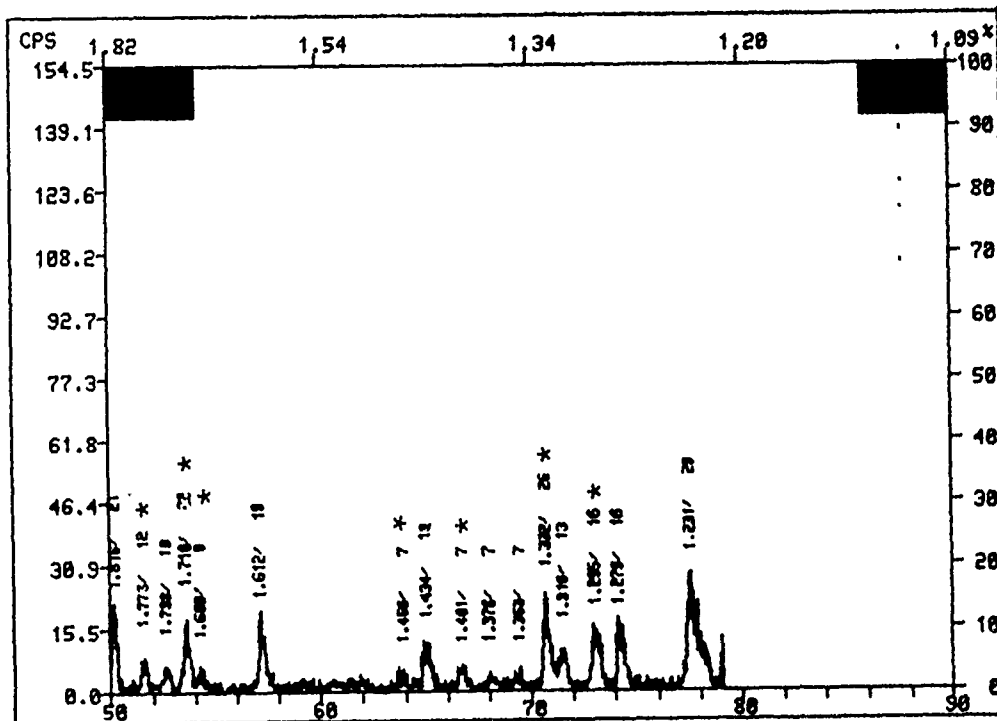


a)

Figure 19. Scanning electron micrograph (a) and x-ray diffraction pattern (b1 and b2) of a $Ti_5Si_3 + Ni$ (33-weight-percent) master alloy (Be-3), 1000X.

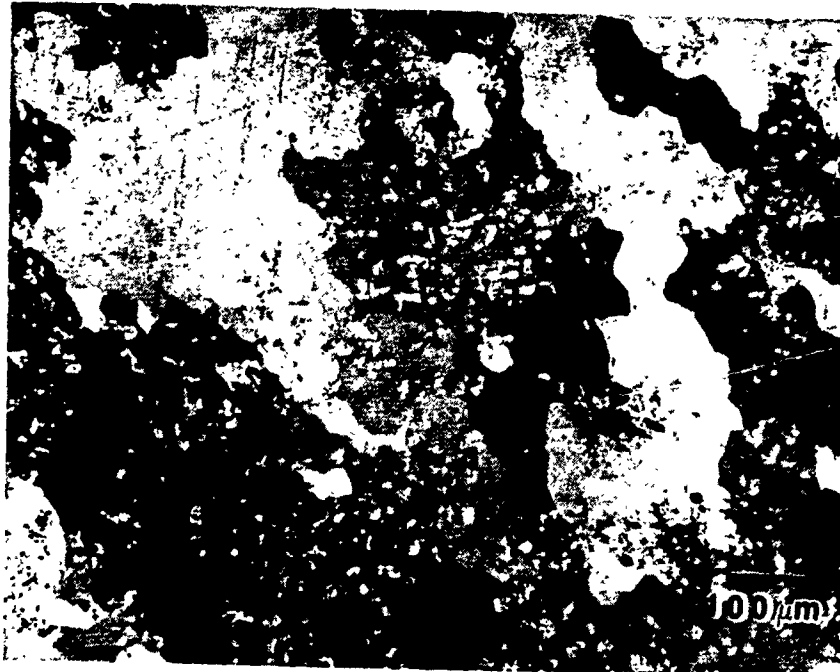


b1)



b2)

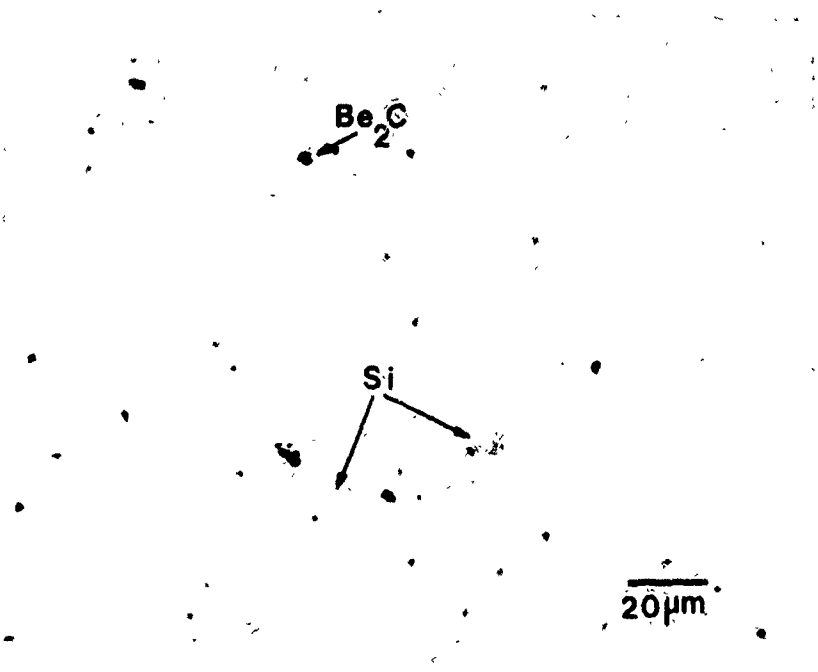
Figure 19. (Continued).



a)

Be-3

POL

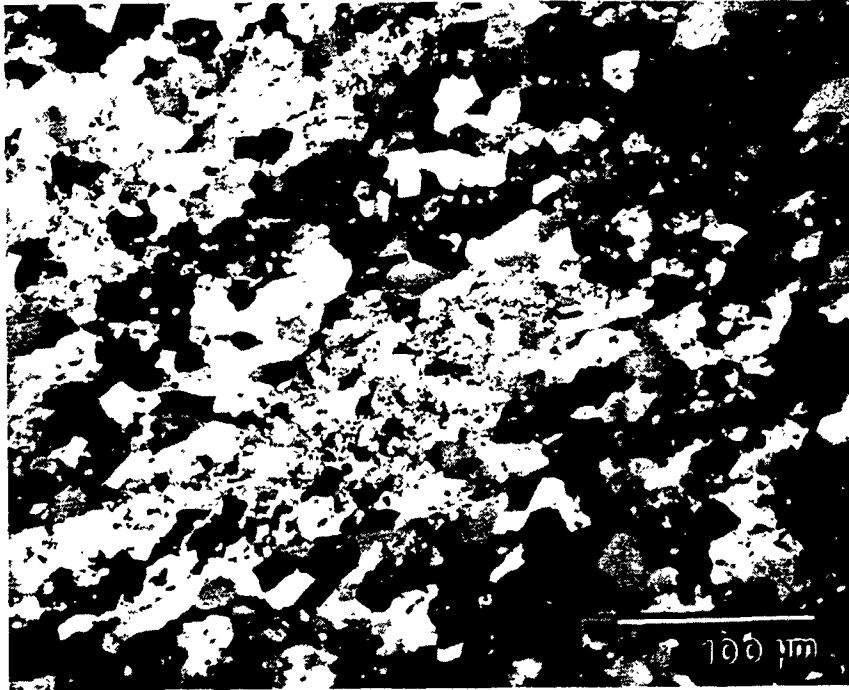


b)

Be-3

BF

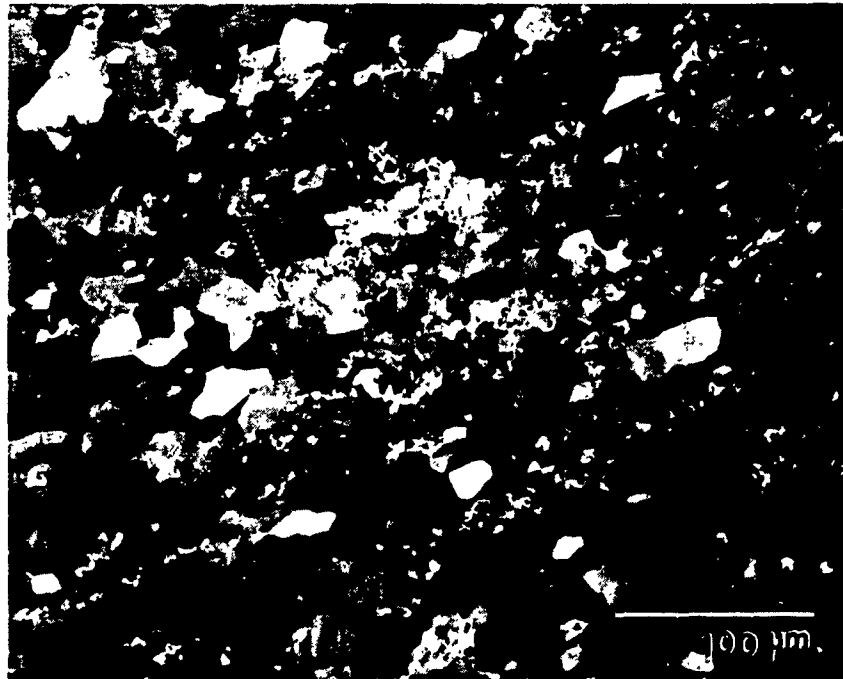
Figure 20. As-cast Be-3: 6-weight-percent Ti_5Si_3 in Ni with a Be matrix.



Rolled Be-3

POL

L-direction



Rolled Be-3

POL

T-direction

Figure 21. Microstructure of cross-rolled Be-3.

XD Master Alloy: This master alloy, consisting of stoichiometric TiO_2/Cu , reacted violently, leaving only 50-percent yield. Despite the vigor, the reaction was only partially complete (small Cu peaks and Cu_2O were identified on the XRD). SEM shows large angular particles (Fig. 22). This morphology is uncommon in XD reactions.

Alloy Billet: The microstructure of casting Be-4 lacked any large particles in the matrix (Fig. 23a). A few Be_2C particles were observed, but no Ti containing intermetallic particles. When this billet was cast, a very large amount of slag was produced. The TiO_2 should have decomposed to BeO and Ti in the melt. The Ti, in the form of oxide or intermetallic, may have segregated into the slag with very little retained in the melt.

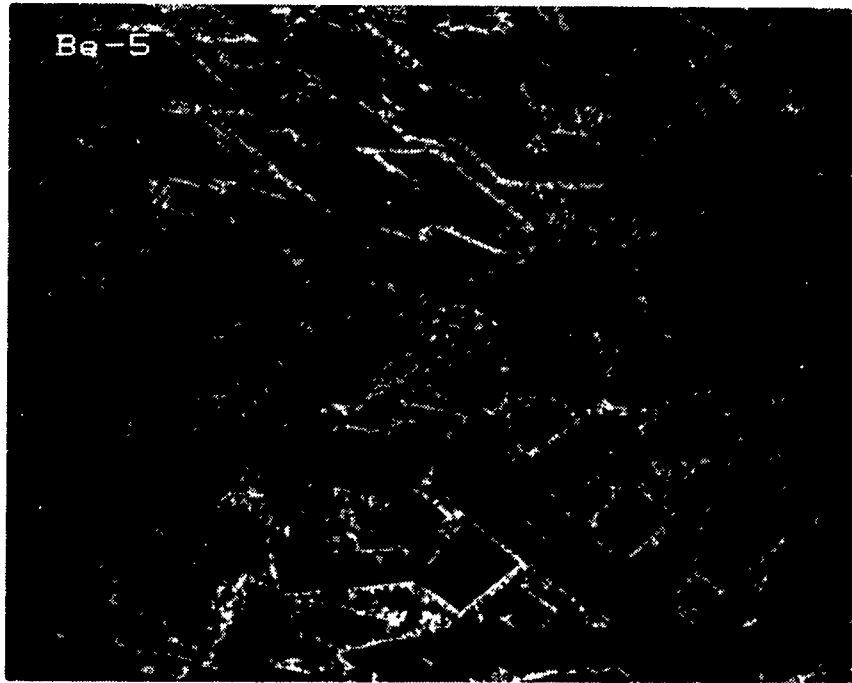
It was noticed that the Be matrix was heavily twinned. Cu additions to Be lower the twinning energy in single Be crystals. With the lack of particles in the Be matrix, twins may have formed in the casting due to cooling stress. It is unclear how particles would suppress twinning in the matrix, but twins were not observed in casting Be-1 or Be-2. Both of these castings also contained Cu.

Rolling Studies: Rolling the cast microstructure produced some grain refinement by producing a more equiaxed grain structure, but the refinement was minimal (Fig. 23b). Twins were also noted in the rolled structure.

F. CASTING Be-5: 10 WEIGHT-PERCENT Ti_5Si_3 IN Ti WITH A Be MATRIX

Predictions: Similar to casting Be-3. Ti_5Si_3 would be reduced by Be, but Ti could react with the Be to form a Ti-beryllide that might stabilize the system.

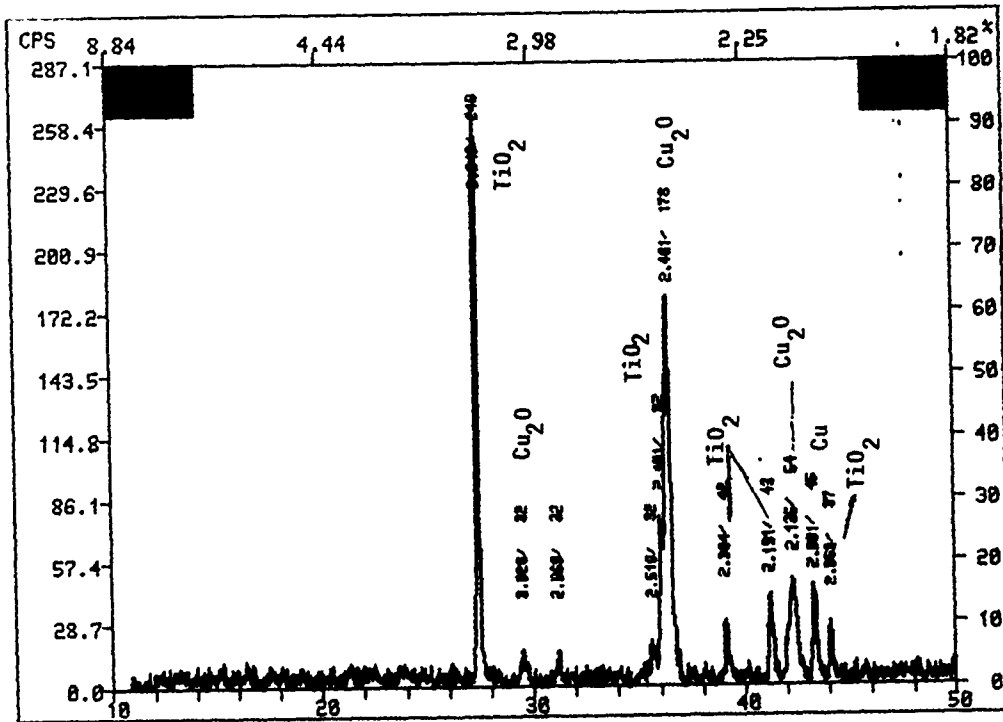
XD Master Alloy: Master alloy Be-4 (33-weight-percent $\text{Ti}_5\text{Si}_3/\text{Ti}$) also reacted cleanly (Fig. 24). This master alloy was formulated to yield 10-volume-percent Ti_5Si_3 in $\text{Ti}_2\text{Be}_{17}$ upon dispersion. The XRD matched well. No micrographs are available.



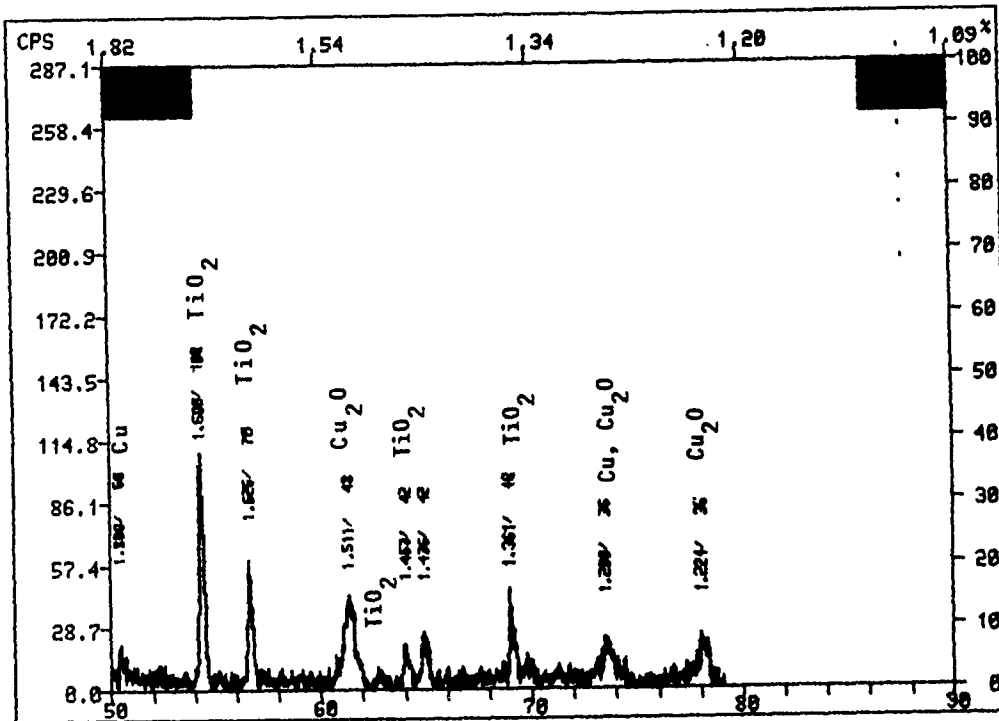
BEI

a)

Figure 22. Scanning electron micrograph (a) and x-ray diffraction pattern (b1 and b2) of a TiO_2 + Cu master alloy (Be-5), 100X.

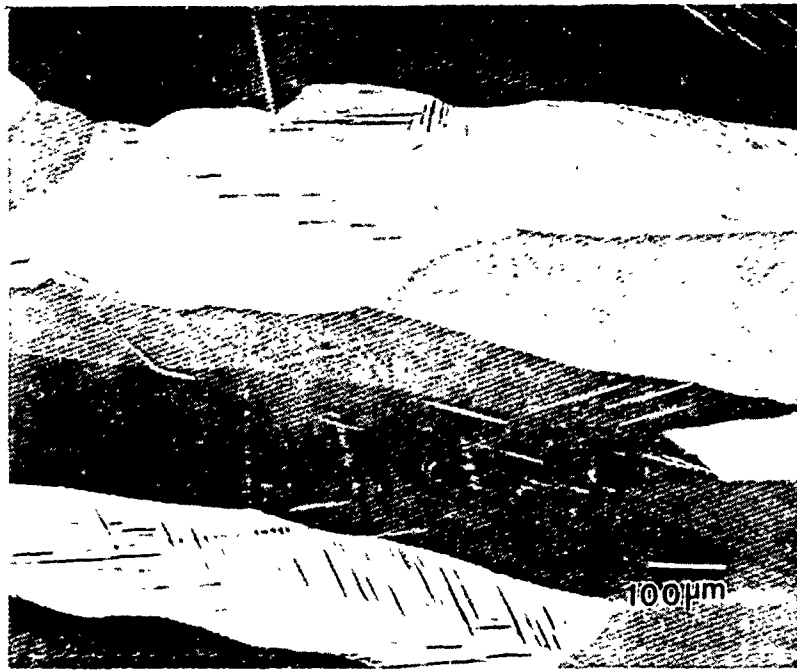


b1)

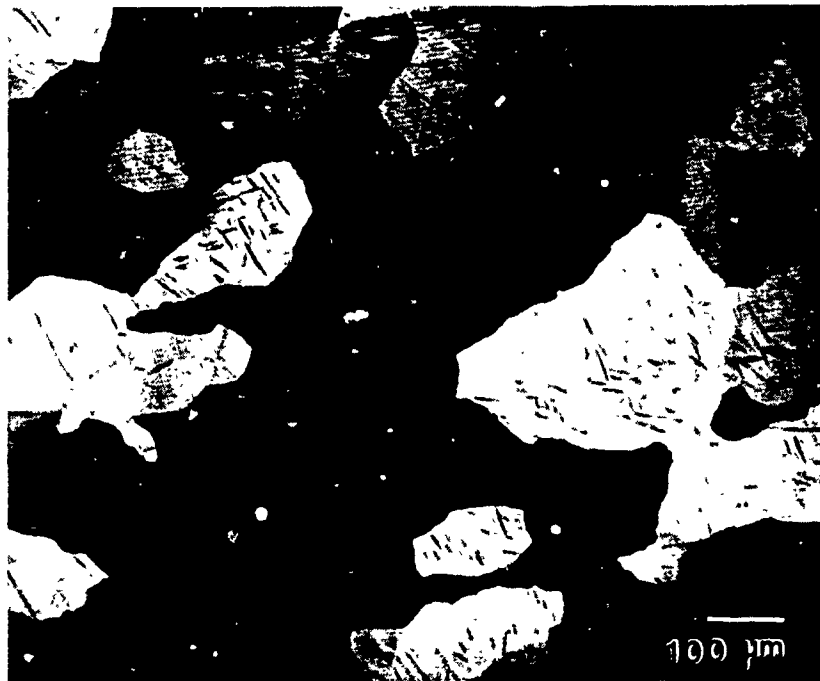


b2)

Figure 22. (Continued).



a) As-cast Be-4 POL



b) Rolled Be-4 POL L-direction

Figure 23. Be-4: 10-weight-percent TiO_2 in Cu with a Be matrix, as-cast and rolled.

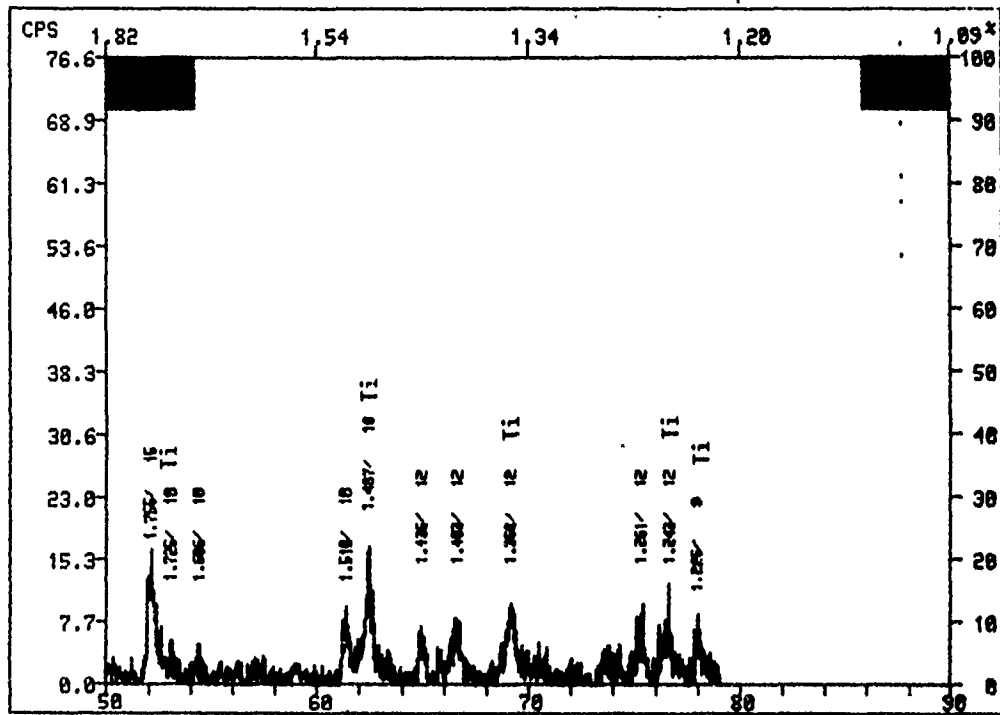
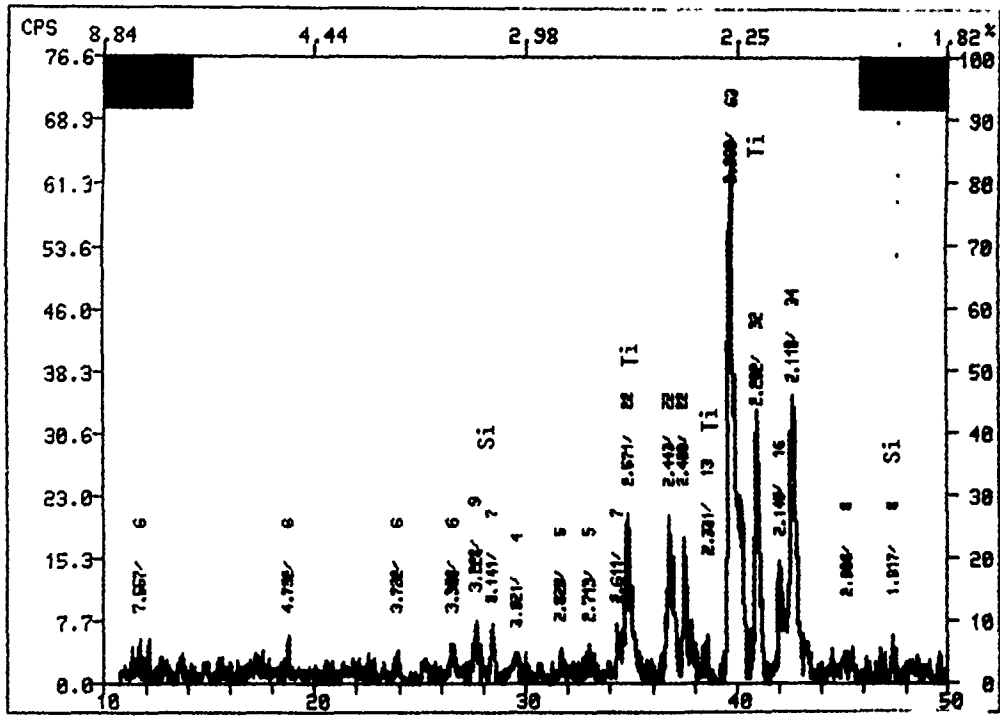


Figure 24. X-ray diffraction pattern for the $Ti_5Si_3 + Ti$ (33-weight-percent) master alloy (Be-4).

Alloy Billet: The microstructure of casting Be-5 was very similar to the other castings using Ti_5Si_3 as a dispersoid, but many more intermetallic particles were observed in the matrix (Fig. 25b). Presumably, this was due to the Ti used as the dispersoid carrier matrix. The grain size of the casting was very large and columnar in morphology.

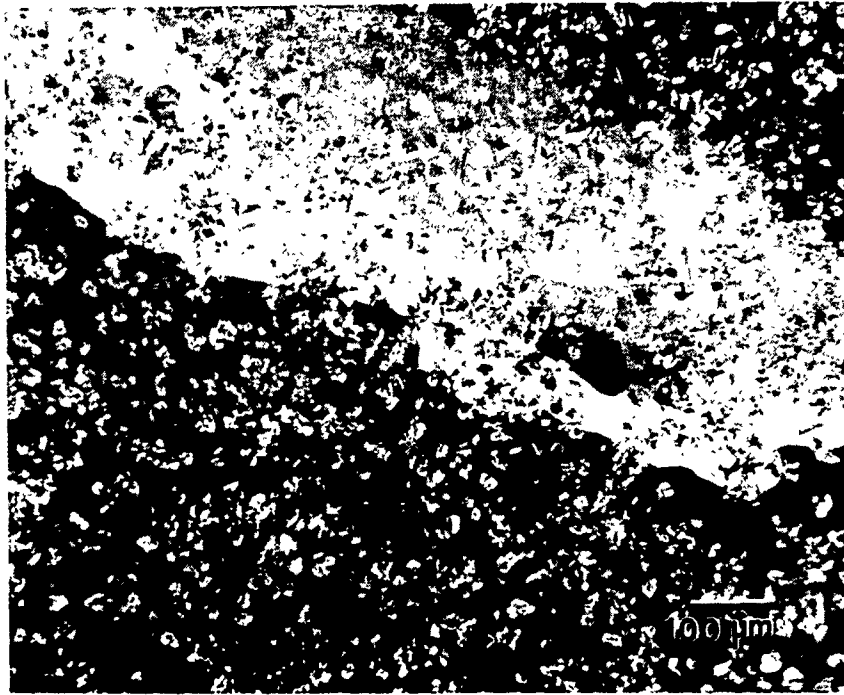
Rolling Studies: Cross-rolling of this microstructure did produce some grain refinement (Fig. 25a). The average grain size was 45 micrometers in the T direction. The intermetallic particles were still well dispersed in the rolled microstructure.

G. CASTING Be-9: 10-WEIGHT-PERCENT $MoSi_2$ IN Cu WITH A Be MATRIX

Predictions: Same as casting Be-2.

XD Master Alloy: Master alloy Be-6 (50-weight-percent $MoSi_2/Cu$) produced a basically clean reaction. Some unidentified peaks on the XRD were seen, probably ternary phases. Photomicrographs show particles in the 1-to-2 micrometer range (Fig. 26). Be-6 was the only $MoSi_2$ alloy used to produce billets. Master alloy Be-10 (65-weight-percent $MoSi_2/Cu$) also reacted cleanly, with some XRD evidence of intermetallics. Although the product was cleaner than master alloy Be-6, the particle sizes varied over a wider range (1 to 8 micrometers by visual inspection) (Fig. 27).

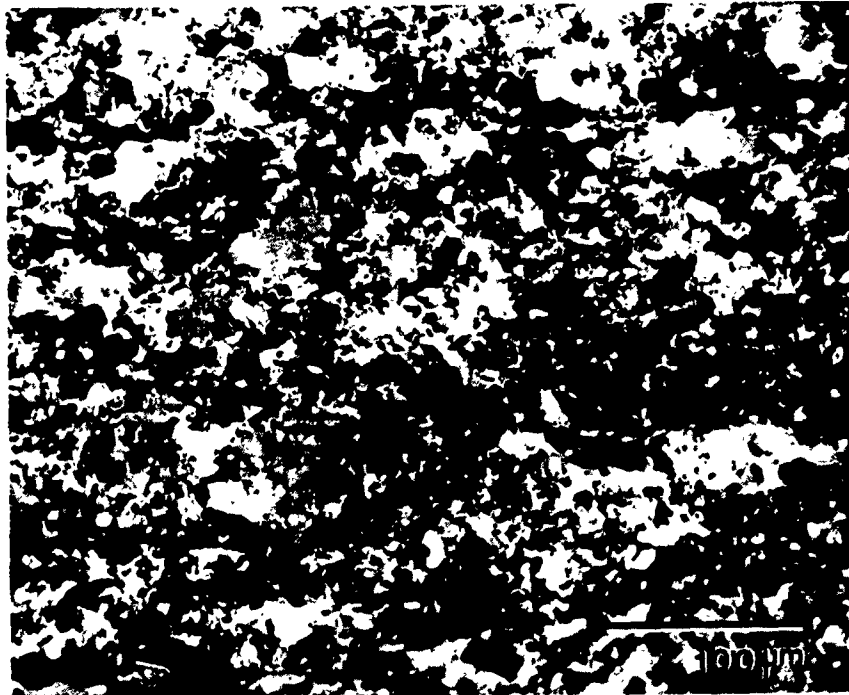
Alloy Billet: The microstructure of casting Be-9 (10-weight-percent $MoSi_2$ in Cu with a Be matrix) is presented in Fig. 28. The grains are heavily twinned, and particles are distributed throughout the matrix. An intercellular phase, identified by EDXA as Si, was also observed in the matrix. It appears that the $MoSi_2$ dispersoid particles decomposed to a Mo-beryllide and elemental Si. Mo-beryllide was not detected by X-ray diffraction, but the volume fraction may be below the threshold of detection for the experimental technique.



a)

As-cast Be-5

POL



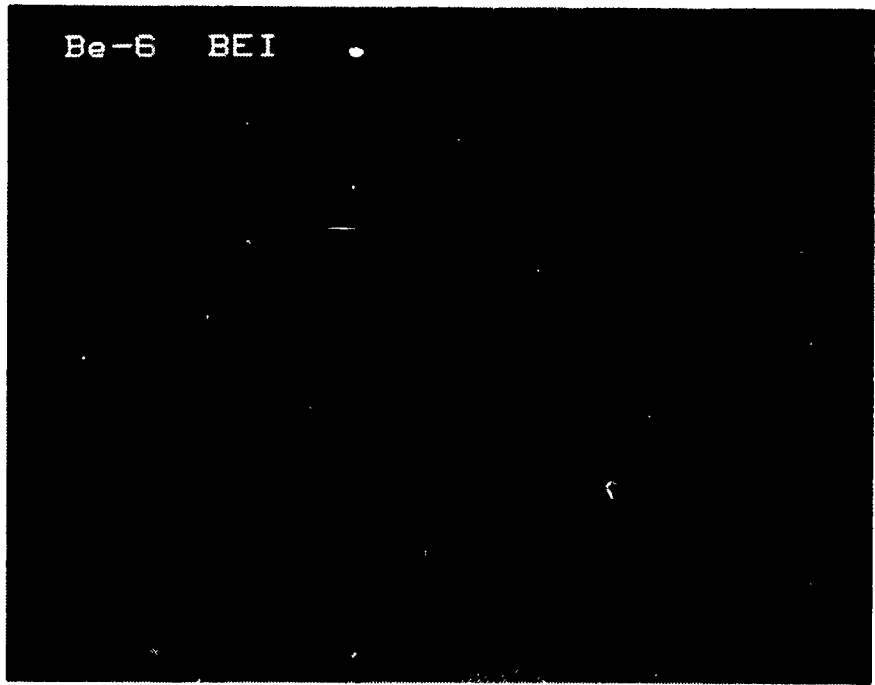
b)

Rolled Be-5

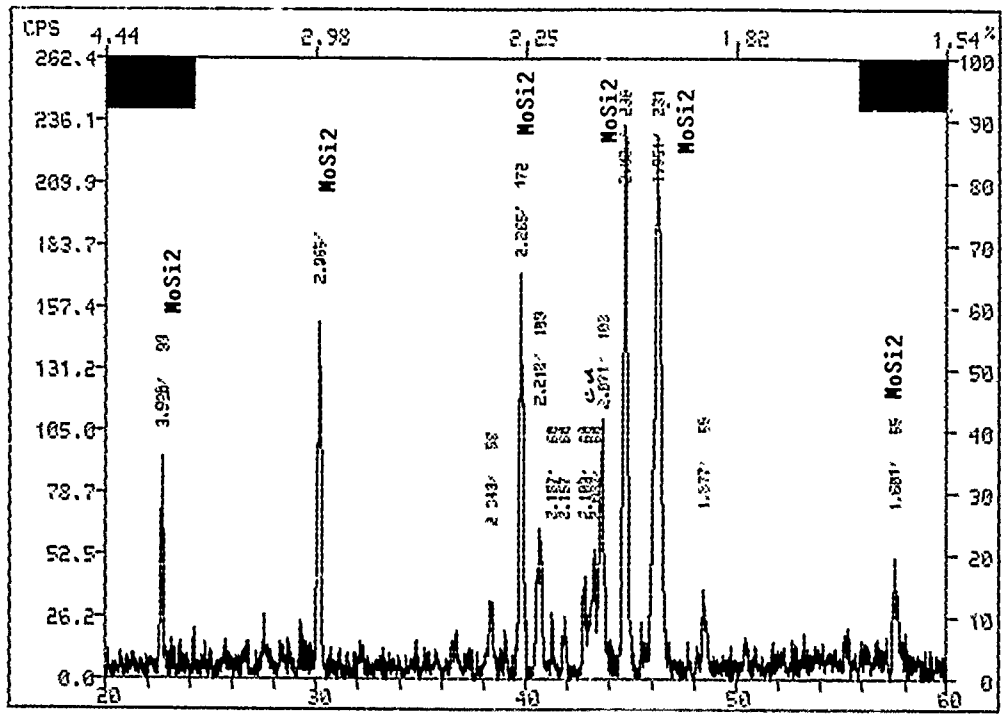
POL

T-direction

Figure 25. Be-5: 10-weight-percent Ti_5Si_3 in Ti with a Be matrix, as-cast and rolled.



a)

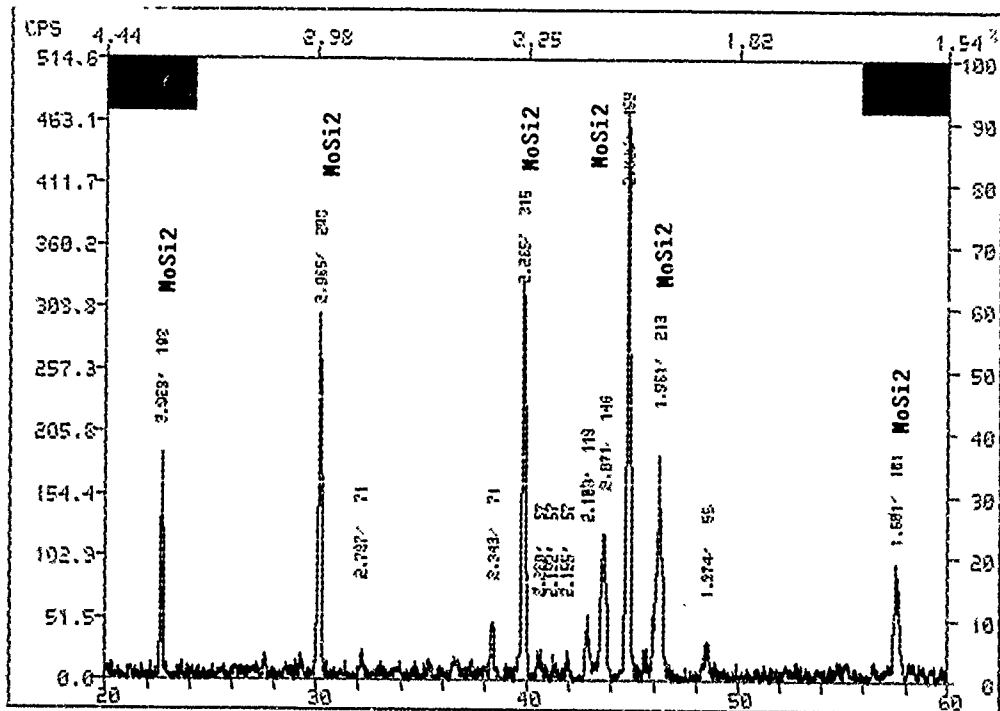


b)

Figure 26. Scanning electron micrograph (a) and x-ray diffraction pattern (b) of a $\text{MoSi}_2 + \text{Cu}$ (65-weight-percent) master alloy (Be-6), 2000X.



a)



b)

Figure 27. Scanning electron micrograph (a) and x-ray diffraction pattern (b) of a $\text{MoSi}_2 + \text{Cu}$ (65 weight-percent) master alloy (Be-10), 2000X.

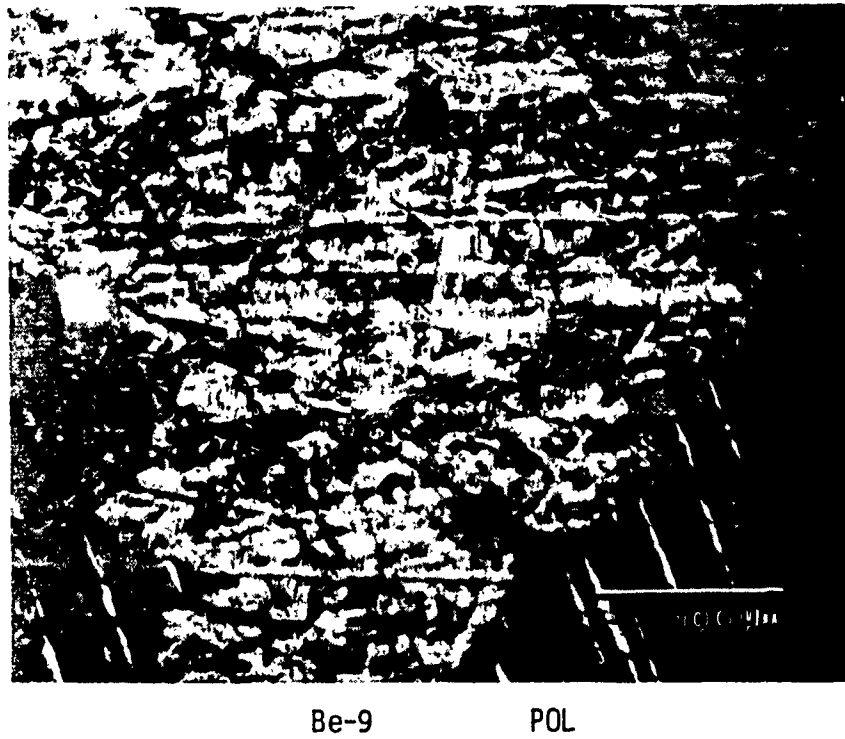
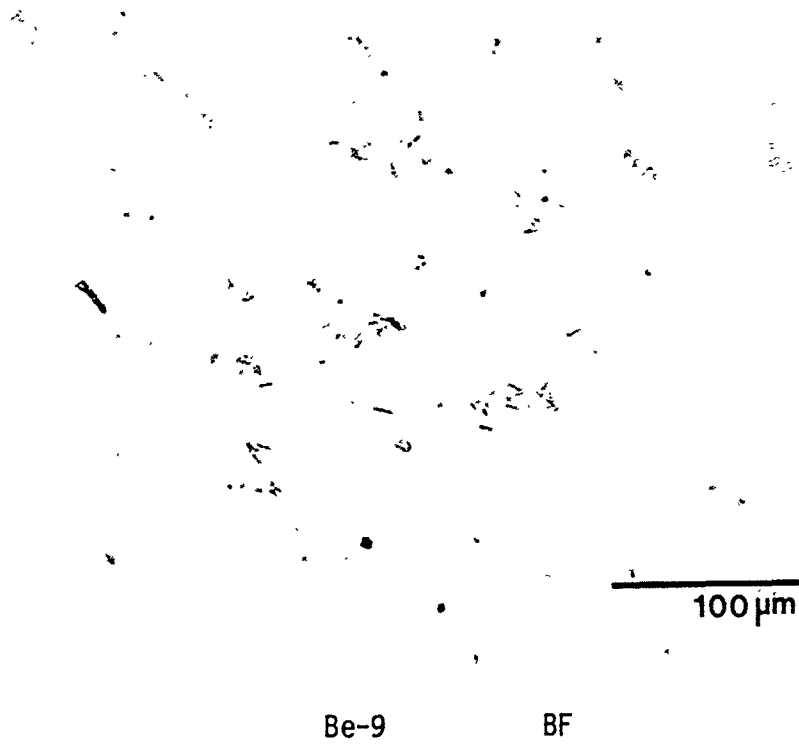


Figure 28. As-cast Be-9: 10 weight-percent MoSi₂ in Cu with a Be matrix.

Rolling Studies: Cross-rolling did both texture and refine the grain size of Be-9, but several of the grains were quite elongated (Fig. 29 & Fig. 30). The beryllide particles were distributed uniformly in the structure, while the Si was located at the grain boundaries.

H. CASTING Be-10: 10-WEIGHT-PERCENT CoAl IN Cu WITH A Be MATRIX

Predictions: It is conceivable that an intermetallic, such as an aluminide, more stable than its conjugate beryllide could be identified and synthesized. Specifically, CoAl is stable in Cu, and if it has a lower free energy than CoBe, it should be stable in Be.

XD Master Alloy: Photomicrographs of master alloy Be-12 (50-weight-percent CoAl/Cu) show a dispersed phase (Fig. 31) that appears to be incompletely reacted. The centers of the particles appear to be unreacted.

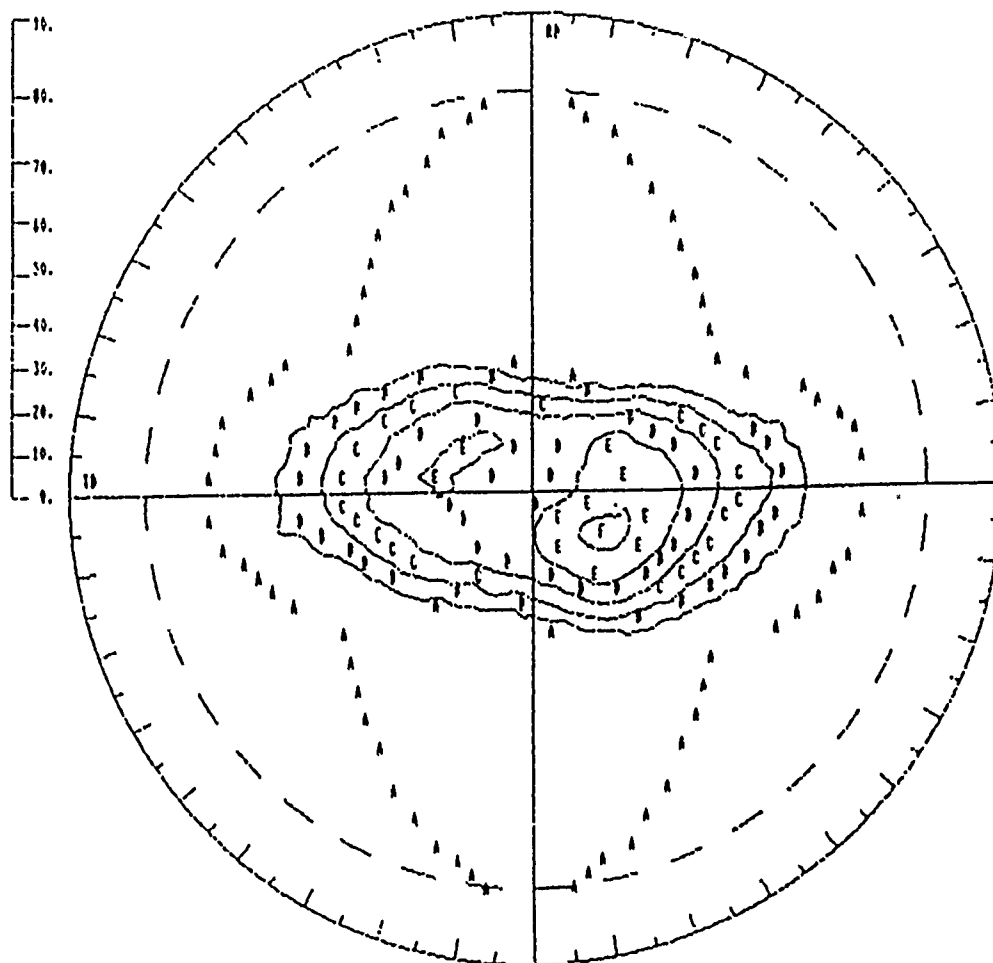
Alloy Billet: Photomicrographs of the microstructure of casting Be-10 are presented in Fig. 32. Fine Co-rich particles can be observed in the matrix. Al is distributed in irregular bodies along cell boundaries. The CoAl dispersoid has decomposed to a Co-beryllide and elemental Al located at cell boundaries. The Cu is in solid solution. The Co-beryllide was not detected by X-ray diffraction, but the volume fraction may be below the threshold of detection.

Rolling Studies: Cross-rolling of casting Be-10 produced some interesting results. The grains became very elongated, and long grain boundary cracks developed in the microstructure. Al could be observed along the cracks and at uncracked grain boundaries. This behavior can be explained by looking at the Be-Al phase diagram. The Be-Al eutectic is at 644°C, well below the rolling temperature. The presence of liquid in the material during rolling caused the sheet to be hot-short. Residual Al is still located at the grain boundaries. Micrographs of the rolled sheet are shown in Fig. 33.

Figure 29

(002) Pole Figure
Stereographic Projection Plot. Times Random Format

Spec. Be-9 Kimm/.5NSPPole



Sym. x RANDOM

A (.00 - .24)
B (.25 - .49)
C (.50 - 1.00)

Sym. x RANDOM

D (1.01 - 2.00)
E (2.01 - 4.00)
F (4.01 - 8.00)

2-Theta = 79.54 deg. Maximum intensity = 3344 Normal intensity = 289
Lambda = 2.29092 Angstroms Background 1 = 77.00 deg. Background 2 = 80.50 deg.

Maximum Times Random = 4.99



Rolled Be-9

POL

L-direction

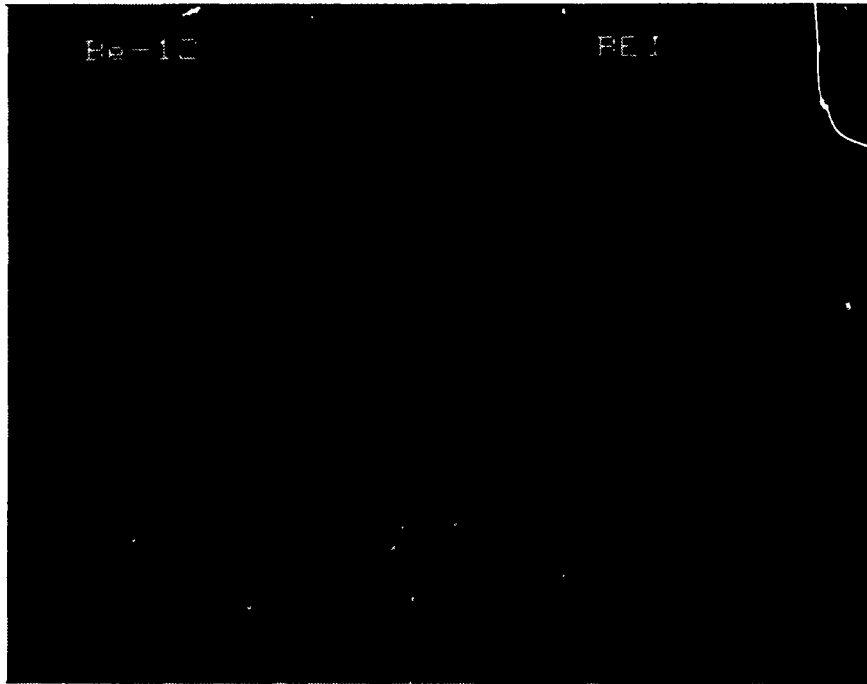


Rolled Be-9

POL

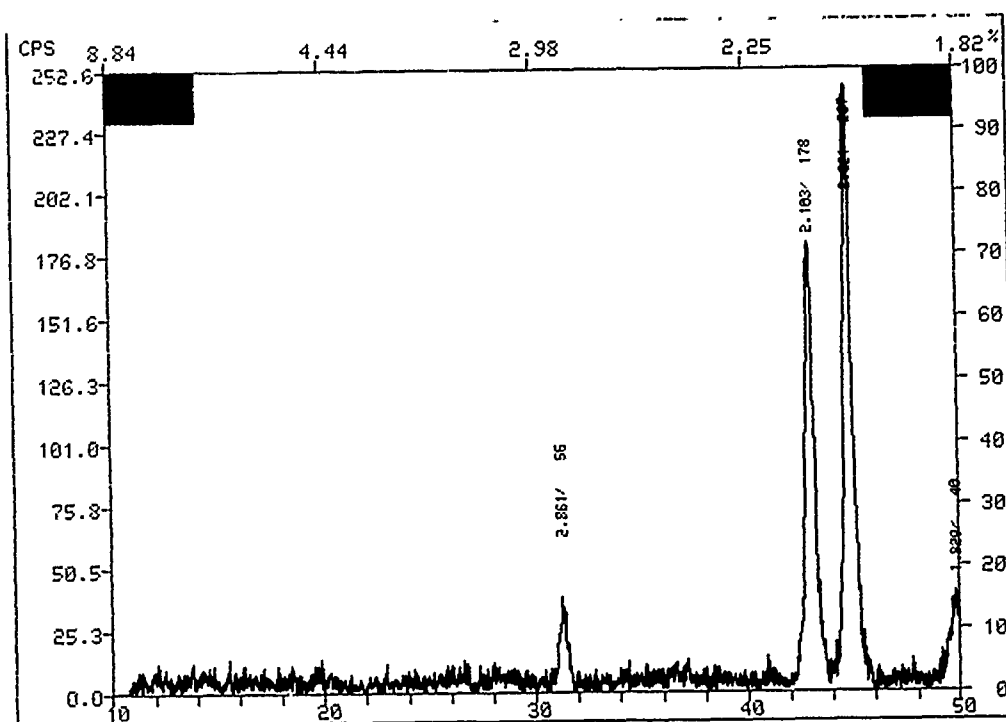
T-direction

Figure 30. Microstructure of cross-rolled Be-9.

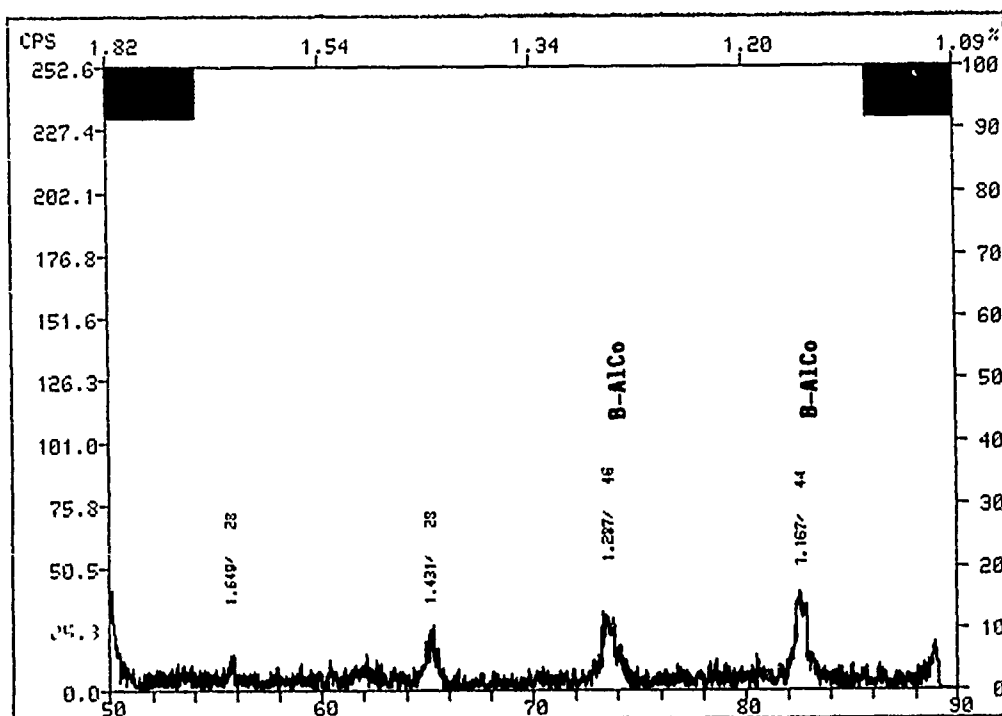


a)

Figure 3]. Scanning electron micrograph (a) and x- ray diffraction pattern (b1 and b2) of a CoAl + Cu (50-weight-percent) master alloy (Be-12), 2000X.



b1)



b2)

Figure 31. (Continued).

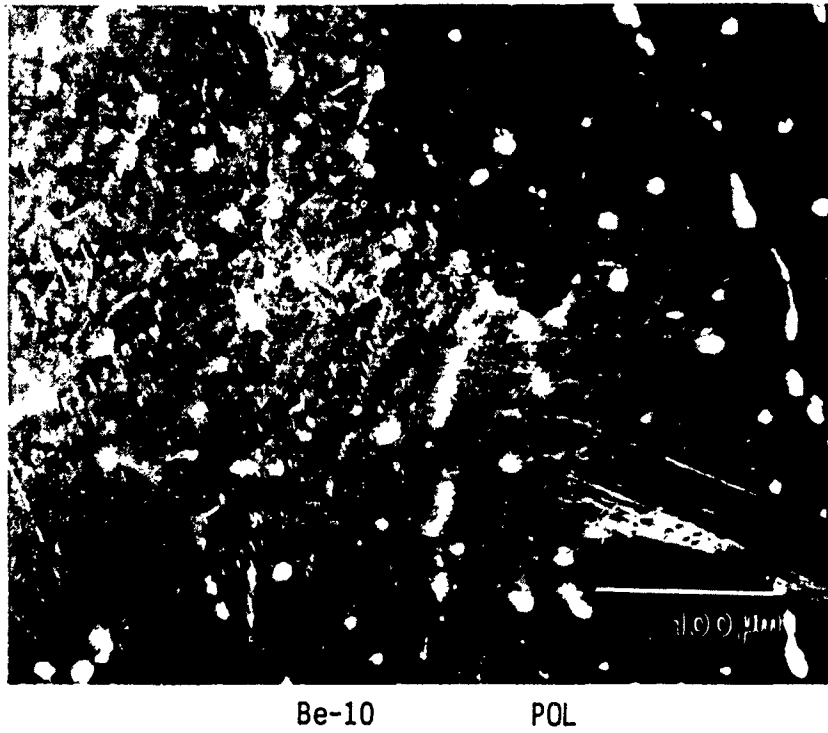
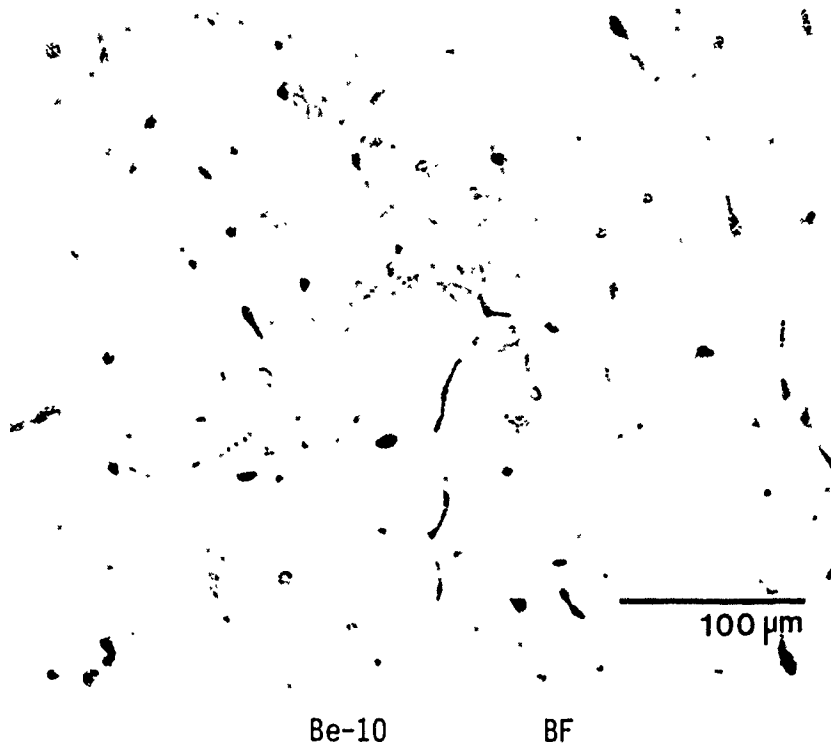
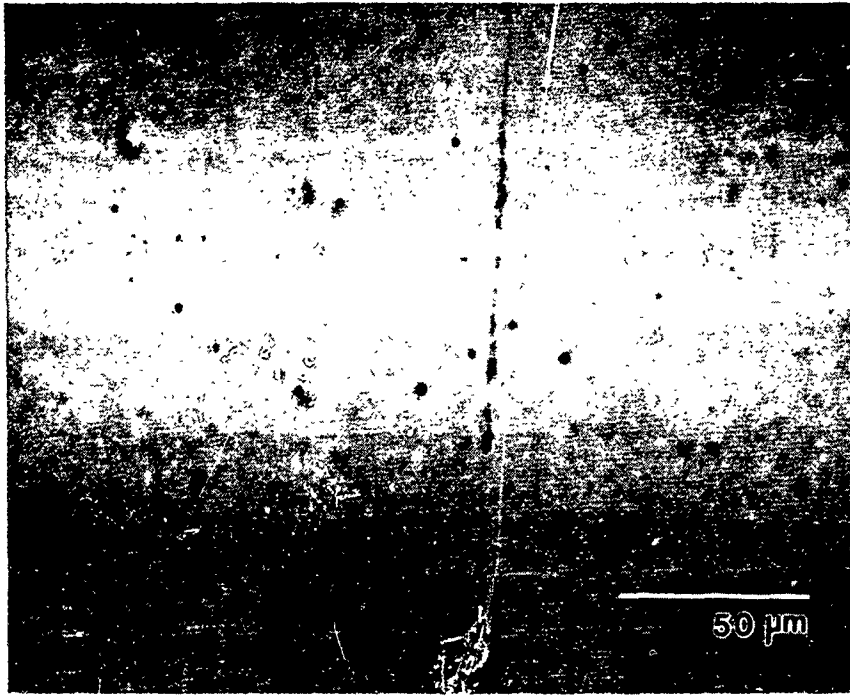
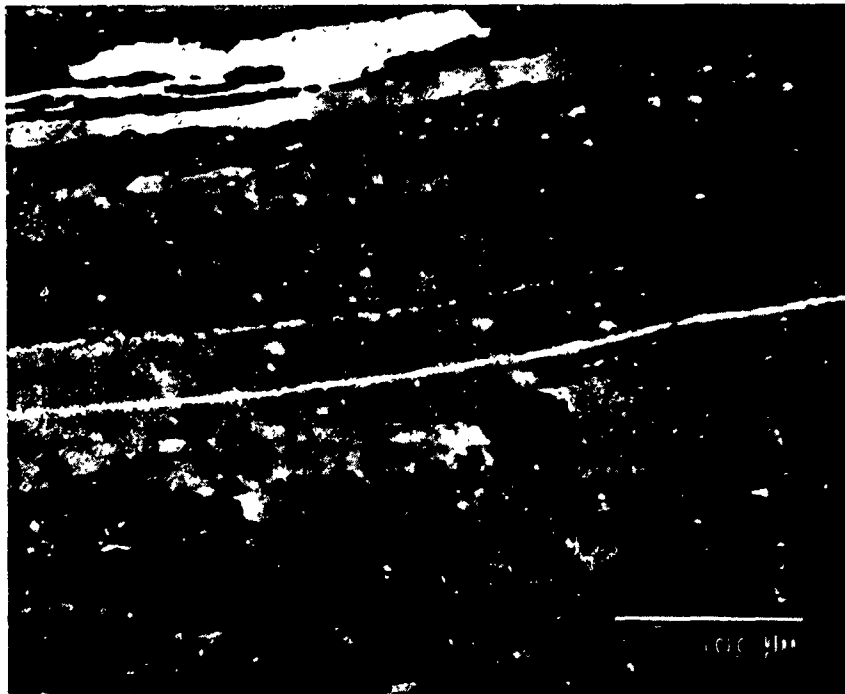


Figure 32. As-cast Be-10: 10-weight-percent CoAl in Cu with a Be matrix.



a) Rolled Be-10 BF L-direction



b) Rolled Be-10 POL T-direction

Figure 33. Microstructure of cross-rolled Be-10.

I. CASTING Be-6: BETA-NiBe CONTROL SAMPLE

Predictions: The nickel beryllides are interesting materials in their own right. The beta phase, nominally NiBe, is cubic and can be rolled into sheet. It also has a broad phase field and is congruent melting, thereby facilitating processing.

XD Master Alloy: Not applicable.

Alloy Billet (Control): The microstructure of cast NiBe is shown in Fig. 34a. The grains were equiaxed in morphology and had an average size of 22 micrometers. Small pores, presumably due to gas, were located throughout the matrix.

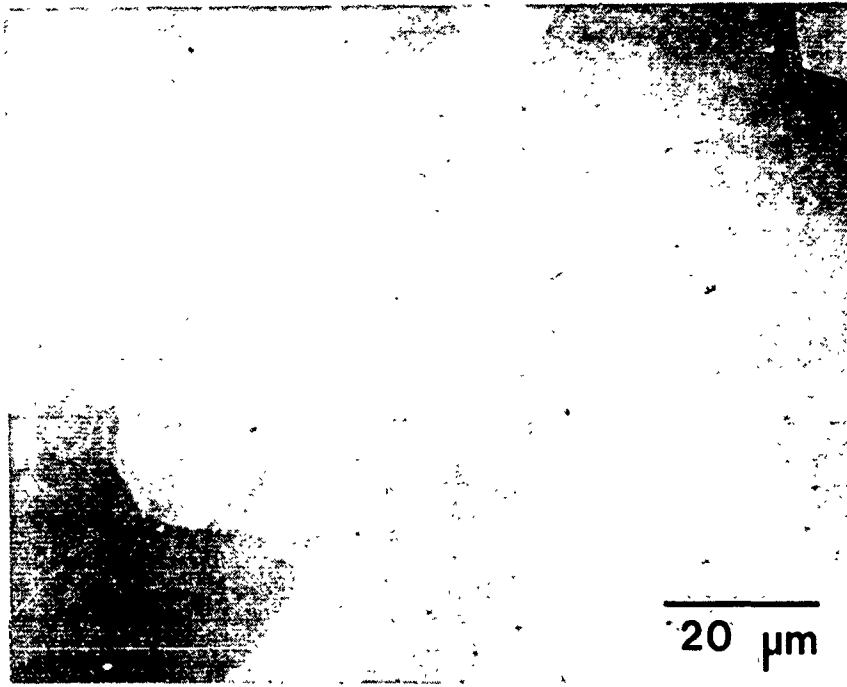
Rolling Studies: Rolling of this casting produced little change in the microstructure. Note that less reduction was experienced by this specimen than by those with a Be matrix. Small subgrains were observed in the grains of the rolled sheet, appearing as bands of slightly different intensity in individual grains. These subgrains are regions of slightly different orientation with a single grain. The differences in orientation show up as slight changes in intensity under polarized light.

J. CASTING Be-7: 10-WEIGHT-PERCENT Ti_5Si_3 IN Cu WITH A NiBe MATRIX

Prediction: Same as beta-NiBe. Additionally, because of the above experience with titanium silicide in a variety of matrices with Be, the beta-NiBe castings were inoculated with Ti_5Si_3 in either Cu or Ni to provide a direct comparison between Be and beta-NiBe.

XD Master Alloy: Same as master alloy Be-2.

Alloy Billet: The microstructure of casting Be-7 is presented in Fig. 35. The microstructure is cellular, with particles dispersed along the cell boundaries. In addition, a phase with a morphology similar to a eutectic was observed at the cell boundaries. Both the matrix and the intercellular phase were optically active, while the particles did not



a)

As-cast Be-6

POL



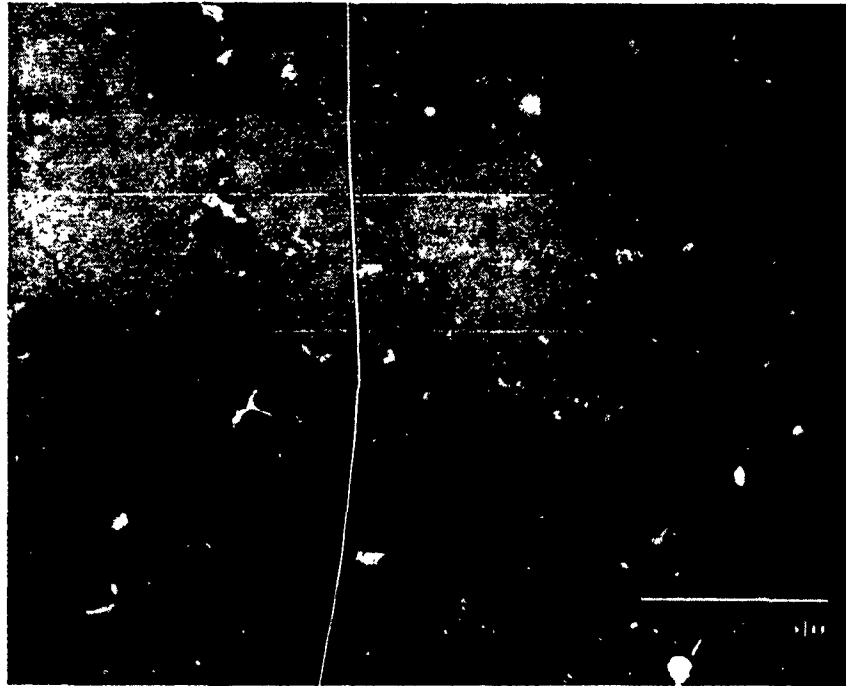
b)

Rolled Be-6

POL

L-direction

Figure 34. Be-6: NiBe, as-cast and rolled.



b)

Be-7

POL

Figure 35. As-cast Be-7: 10-weight-percent Ti_5Si_3 in Cu with a NiBe matrix.

appear to be optically active. The intercellular regions were enriched in Cu. The phase may be a Ni or Cu-Be eutectic. Further study is required to determine the nature and formation of the phase.

Rolling Studies: Attempts to produce rolling blocks from this casting were not successful. The billet cracked and an acceptable rolling block could not be fabricated. Alternative methods to machine a rolling block, such as EDM or chemical sawing, were not attempted but may be successful with this material.

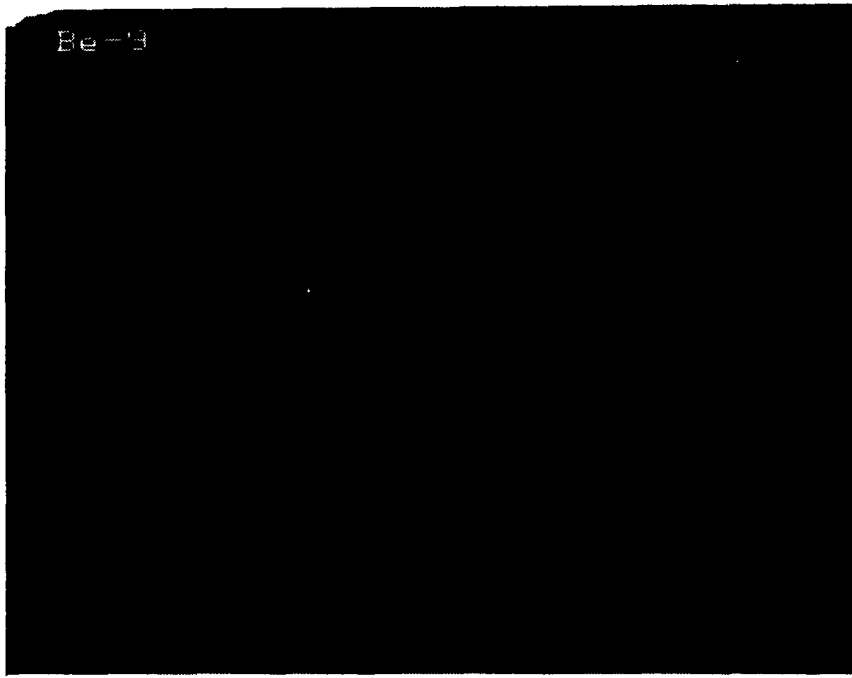
K. CASTING Be-8: 10-WEIGHT-PERCENT Ti_5Si_3 IN Ni WITH A NiBe MATRIX

Predictions: Same as for casting Be-7.

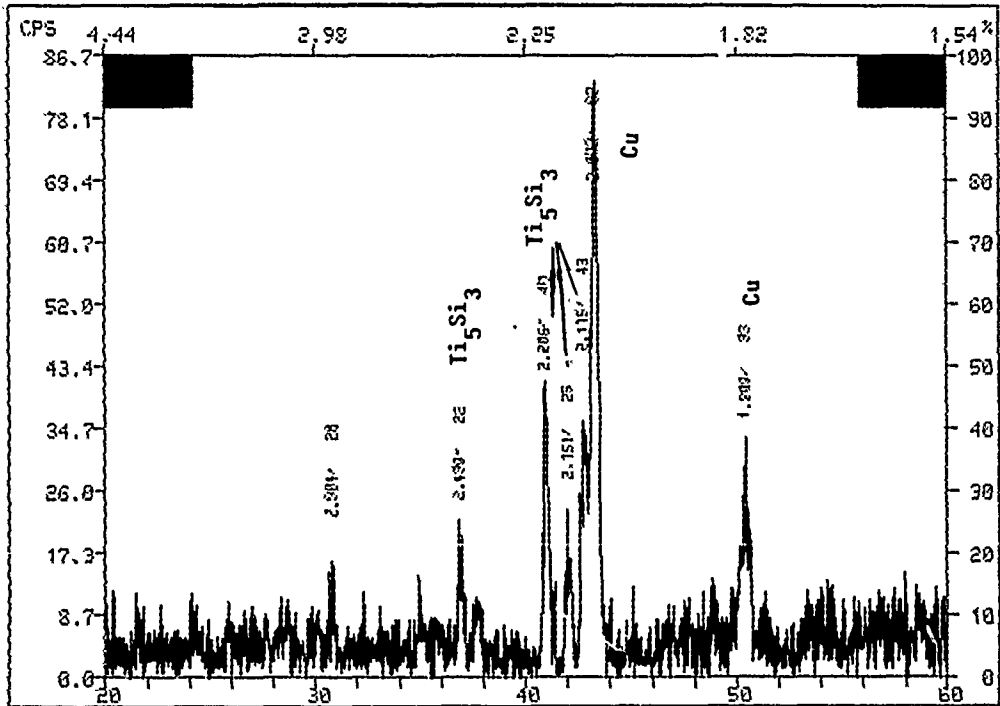
XD Master Alloy: Same as master alloy Be-2. Master alloy Be-9 had lower levels of $Ni_{16}Ti_6Si_7$ than its 50-percent counterpart. SEM showed a large angular second phase (Fig. 36).

Alloy Billet: The microstructure of casting Be-8 is presented in Fig. 37. The microstructure is identical to casting Be-7. Be-8 has a cellular microstructure, with particles and a cellular eutectic distributed along the cell boundaries. Be_2C was also observed in the matrix.

Rolling Studies: As with casting Be-7, attempts to produce rolling blocks from this casting were not successful.

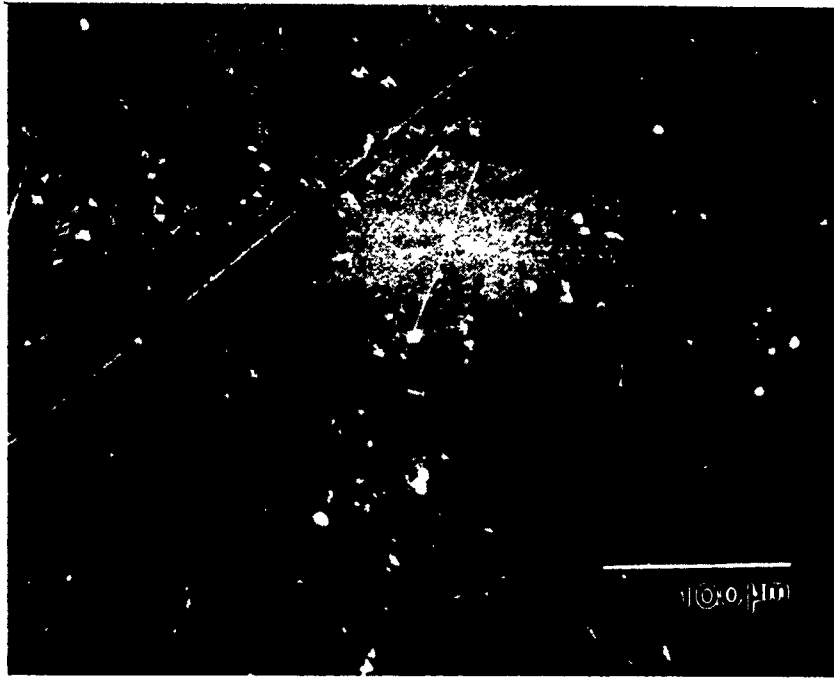


a)



b)

Figure 36. Scanning electron micrograph (a) and x-ray diffraction pattern (b) of a $Ti_5Si_3 + Ni$ (70-weight-percent) master alloy (Be-9), 1000X.



b)

Be-8

POL

Figure 37. As-cast Be-8: 10-weight-percent Ti_5Si_3 in Ni with a NiBe matrix.

IV. CONCLUSIONS

Eleven beryllium castings were made by Brush Wellman using dispersoid materials provided by Martin Marietta Laboratories. Eight castings had a beryllium matrix, while three had a NiBe matrix. Each casting was analyzed metallographically. It was found that all the selected dispersoid materials reacted with the beryllium matrix. Little grain refinement was observed in the castings. Slabs cut from the cast billets were rolled to produce sheet. It was found that the grain size of the rolled material was only slightly finer than a pure Be control sample.

XD materials can be successfully incorporated in beryllium, but they have little effect on the as-cast grain size. Some refinement in the rolled structure was observed. Other observations:

- 1) Several different methods of incorporating the XD material into the beryllium were used, the most successful being to place the XD material on the surface of the Be lump prior to melting. The Be melted first and then dissolved the XD material. Excessive slag resulted from other inoculation methods.
- 2) The Be castings had large amounts of solidification shrinkage. Directional solidification of the molten metal should solve the problem.
- 3) The Be-based billets were easily machined. Only the NiBe billet could be sectioned; the other NiBe billets containing dispersoids could not be cut without cracking.
- 4) Cross-rolling of the cast material was generally successful. Several of the billets cracked on rolling. Casting Be-10, which contained free Al, exhibited hot shortness (see 9 below).
- 5) Microstructural examination of the billets revealed that no dispersoid remained intact; all had reacted with the Be and were transformed to other phase(s).

- 6) The carrier metals, Cu, Ni, or Ti, did not have a noticeable effect on dispersoid reactivity. Cu additions did tend to promote matrix twinning.
- 7) Be_2C was a contaminant in all of the XD castings.
- 8) Cross-rolling did result in a reduction of the grain size in several of the cast materials. The rolling operation also caused the intermetallic particles to crack. The degree of texturing was lower than that observed for powder sheet material subjected to similar mechanical working by rolling.
- 9) Casting Be-10, which contained free aluminum after the decomposition of CoAl by the Be matrix, exhibited hot shortness during cross-rolling. The Al was molten during the rolling process and weakened the grain boundaries, causing the rolling block to crack.
- 10) Limited mechanical property tests indicate that the XD materials did not produce increased tensile properties. The strain to failure for the XD material was greater than that of the control indicating increased brittleness.

REFERENCES

1. H.H. Hausner, Beryllium: Its Metallurgy and Properties, University of California Press, Berkeley, CA.
2. D. Webster and D.D. Crooks, Improved Beryllium Ductility Study, Final Report on Contract No. N60921-74-C-0114.
3. J.W. Moberly, O.D. Sherby, and J.C. Shyne, Investigation of Beryllium with Added Dispersoids, AFML-TR-69-247.
4. Phase Diagrams of Binary Titanium Alloys, J.L. Murray, ed., ASM International, Metals Park, OH, 1987.
5. Phase Diagrams of Binary Beryllium Alloys, H. Okamoto and L. Tanner, eds., ASM International, Metals Park, OH, 1987.